REVIEWS SCIENCE CHINA Materials

mater.scichina.com link.springer.com

Published online 17 December 2014 | doi: 10.1007/s40843-014-0003-1
Sci China Mater 2014, 57: 70–100

Design and fabrication of semiconductor photocatalyst for photocatalytic reduction of CO_2 to solar fuel

Xin Li[1,2], Jiuqing Wen[2], Jingxiang Low[1], Yueping Fang[2] and Jiaguo Yu[1,3*]

The shortage of fossil fuels and the disastrous pollution of the environment have led to an increasing interest in artificial photosynthesis. The photocatalytic conversion of CO_2 into solar fuel is believed to be one of the best methods to overcome both the energy crisis and environmental problems. It is of significant importance to efficiently manage the surface reactions and the photo-generated charge carriers to maximize the activity and selectivity of semiconductor photocatalysts for photoconversion of CO_2 and H_2O to solar fuel. To date, a variety of strategies have been developed to boost their photocatalytic activity and selectivity for CO_2 photoreduction. Based on the analysis of limited factors in improving the photocatalytic efficiency and selectivity, this review attempts to summarize these strategies and their corresponding design principles, including increased visible-light excitation, promoted charge transfer and separation, enhanced adsorption and activation of CO_2, accelerated CO_2 reduction kinetics and suppressed undesirable reaction. Furthermore, we not only provide a summary of the recent progress in the rational design and fabrication of highly active and selective photocatalysts for the photoreduction of CO_2, but also offer some fundamental insights into designing highly efficient photocatalysts for water splitting or pollutant degradation.

INTRODUCTION

The shortage of the energy supply and the problem of disastrous environmental pollution have been recognized as two main challenges in the near future [1]. It is a better way to efficiently and inexpensively convert solar energy into chemical fuels by developing an artificial photosynthetic (APS) system because solar fuels are high density energy carriers with long-term storage capacity. The most important and challenging reactions in APS—the photocatalytic water splitting into H_2 and O_2 (water reduction and oxidation) [2–4] and photoreduction of CO_2 to solar fuel, such as CH_4 and CH_3OH [5,6] have been extensively studied since the photocatalytic water splitting on TiO_2 electrodes was discovered by Honda and Fujishima in 1972 [7]. The photocatalytic reduction of CO_2 by means of solar energy has attracted growing attention in the recent years, which is also believed to be one of the best methods to overcome both global warming and energy crisis [8]. However, it is also generally thought that photocatalytic CO_2 reduction is a more complex and difficult process than H_2 production due to preferential H_2 production and low selectivity for the carbon species produced [9,10]. The progress achieved in the photoreduction of CO_2 is still far behind that in water splitting for a few decades because of the low efficiency and selectivity, and limited photocatalysts [11,12]. Therefore, there is an urgent need for artificial photosynthesis research to focus on the formidable challenge of converting CO_2 and water into valuable hydrocarbons or liquid fuels.

Up to now, many different heterogeneous [4,13,14] and homogeneous [15] photocatalysts have been extensively studied in the different fields of photocatalysis over the past decades. Extensive research has been underway to develop highly heterogeneous photocatalysts for the application of semiconductor photocatalysis because heterogeneous systems have more advantages and a wider range of potential applications than the homogeneous systems [2,13,16]. From the viewpoint of searching for suitable photocatalysts, a number of reviews about various TiO_2 and non-TiO_2 heterogeneous semiconductor photocatalyst materials used in the fields of photocatalytic reduction of CO_2 have been available [17–19]. However, most of them only focus on the review of various kinds of semiconductor photocatalysts, there are few reviews about the design strategies for the fabrication of highly efficient photocatalysts [20]. Besides continuous fabrication of new visible-light-driven photocatalysts, it is also a very important topic to enhance the selectivity, stability and activity of existing photocatalysts for CO_2 photoreduction. Furthermore, it is clear that photo-generated charge carriers and surface reactions play very important roles in enhancing the overall efficiency for CO_2 photoreduction. Thus, it is also significant to efficiently manage the photo-generated charge carriers and surface reactions of semiconductor photocatalysts to maximize the activity and selectivity for conversion of solar energy and CO_2 to fuel. Any processes consuming photo-gener-

[1] State Key Laboratory of Advanced Technology for Material Synthesis and Processing, Wuhan University of Technology, Wuhan 430070, China
[2] College of Science, South China Agricultural University, Guangzhou 510642, China
[3] Department of Physics, Faculty of Science, King Abdulaziz University, Jeddah 21589, Saudi Arabia
[*] Corresponding author (email: jiaguoyu@yahoo.com)

ated electrons and undesirable reactions will decrease the overall efficiency, which should be weakened or completely avoided. In addition, the kinetic challenges are great owing to the complex multi-electron reduction processes of CO_2 [21,22]. Thus, increasing the kinetics of CO_2 reduction is a critical step to enhance the overall efficiency. Therefore, this review will focus on the design of highly selective and efficient semiconductor photocatalysts for CO_2 photoreduction through a rational management of photo-generated charge carriers and surface reactions. Various strategies and their corresponding design principles are summarized here, including increased visible-light excitation, promoted charge transfer and separation, enhanced adsorption and activation of CO_2, accelerated CO_2 reduction kinetics and suppressed undesirable reaction. This review not only differs from the previous reviews focusing on the summarization of various photocatalysts for CO_2 photoreduction, but also is different from the reviews about the typical design strategies applied in the water splitting and organic pollutants degradation due to the complexity of the carbon species from CO_2 reduction [23,24]. It may open a new opportunity for designing highly effective photocatalysts for both CO_2 reduction and water splitting.

FUNDAMENTALS OF PHOTOCATALYTIC CO_2 REDUCTION

Thermodynamics of photocatalytic CO_2 reduction

The free energy ΔG^0 and the standard redox potential ΔE^0 of the multi-electron water splitting (Equation (1)) and CO_2 reduction (Equation (2–6)) are listed in Equation (1–6) [25]. The ΔG^0 values of all the reactions are highly positive, and make CO_2 reduction a highly endothermic process which is much more difficult to proceed at ambient temperature. The ΔG^0 values also indicate that the CO_2 reduction reactions can store more energy than the water splitting reaction [25,26].

$$H_2O(l) \rightarrow H_2(g) + 1/2O_2(g),$$
$$\Delta G0 = 237\ \text{kJ/mol}, \Delta E0 = 1.23\ \text{V}. \quad (1)$$

$$CO_2(g) \rightarrow CO(g) + 1/2O_2(g),$$
$$\Delta G^0 = 257\ \text{kJ/mol}, \Delta E^0 = 1.33\ \text{V}. \quad (2)$$

$$CO_2(g) + H_2O(l) \rightarrow HCOOH(l) + 1/2O_2(g),$$
$$\Delta G^0 = 286\ \text{kJ/mol}, \Delta E^0 = 1.48\ \text{V}. \quad (3)$$

$$CO_2(g) + H_2O(l) \rightarrow HCHO(l) + O_2(g),$$
$$\Delta G^0 = 522\ \text{kJ/mol}, \Delta E^0 = 1.35\ \text{V}. \quad (4)$$

$$CO_2(g) + 2H_2O(l) \rightarrow CH_3OH(l) + 3/2O_2(g),$$
$$\Delta G^0 = 703\ \text{kJ/mol}, \Delta E^0 = 1.21\ \text{V}. \quad (5)$$

$$CO_2(g) + 2H_2O(l) \rightarrow CH_4(g) + 2O_2(g),$$
$$\Delta G^0 = 818\ \text{kJ/mol}, \Delta E^0 = 1.06\ \text{V}. \quad (6)$$

For reduction of CO_2, the reaction by one electron to form CO_2^- radical is highly unfavorable due to the higher reduction potential of −1.9 V *vs.* normal hydrogen electrode (NHE). In addition, a large kinetic "overvoltage" for the one-electron reduction was required because of the structural differences between linear CO_2 and bent CO_2^- [15,26,27]. In contrast, the multi-electronic processes are more favorable, which require much less energy for per electron transfer as compared to mono-electron process. The standard reduction potentials of CO_2 for the half-cell reactions are summarized in Table 1 (at pH 7 in aqueous solution *vs.* NHE) [15,22,26–30]. Fig. 1 shows a Latimer–Frost diagram for the multi-electron, multi-proton reduction of CO_2 in aqueous solution at pH 7 [31]. As depicted in Fig. 1, the slope derived from each blue dashed line represents the standard redox potential of the corresponding multi-electron CO_2 reduction reaction. It can be clearly seen from Table 1 and Fig. 1 that proton-assisted, multi-electron approach to CO_2 reduction lowers the thermodynamic barrier significantly [31]. Furthermore, every

Table 1 Reduction potentials of CO_2

Reaction	E^0 (V) *vs.* NHE at pH 7
Reduction potentials of CO_2	
$2H^+ + 2e^- \rightarrow H_2$	−0.41
$CO_2 + e^- \rightarrow CO_2^-$	−1.9
$CO_2 + 2H^+ + 2e^- \rightarrow HCO_2H$	−0.61
$CO_2 + 2H^+ + 2e^- \rightarrow CO + H_2O$	−0.53
$CO_2 + 4H^+ + 4e^- \rightarrow C + 2H_2O$	−0.2
$CO_2 + 4H^+ + 4e^- \rightarrow HCHO + H_2O$	−0.48
$CO_2 + 6H^+ + 6e^- \rightarrow CH_3OH + H_2O$	−0.38
$CO_2 + 8H^+ + 8e^- \rightarrow CH_4 + 2H_2O$	−0.24
$2CO_2 + 8H_2O + 12e^- \rightarrow C_2H_4 + 12OH^-$	−0.34
$2CO_2 + 9H_2O + 12e^- \rightarrow C_2H_5OH + 12OH^-$	−0.33
$3CO_2 + 13H_2O + 18e^- \rightarrow C_3H_7OH + 18OH^-$	−0.32
Reduction potentials of H_2CO_3	
$2H^+ + 2e^- \rightarrow H_2$	−0.41
$2H_2CO_3 + 2H^+ + 2e^- \rightarrow H_2C_2O_4 + 2H_2O$	−0.8
$H_2CO_3 + 2H^+ + 2e^- \rightarrow HCOOH + H_2O$	−0.576
$H_2CO_3 + 4H^+ + 4e^- \rightarrow HCHO + 2H_2O$	−0.46
$H_2CO_3 + 6H^+ + 6e^- \rightarrow CH_3OH + 2H_2O$	−0.366
$H_2CO_3 + 4H^+ + 4e^- \rightarrow C + 3H_2O$	−0.182
Reduction potentials of CO_3^{2-}	
$2H^+ + 2e^- \rightarrow H_2$	−0.41
$2CO_3^{2-} + 4H^+ + 2e^- \rightarrow C_2O_4^{2-} + 2H_2O$	0.07
$CO_3^{2-} + 3H^+ + 2e^- \rightarrow HCOO^- + H_2O$	−0.099
$CO_3^{2-} + 6H^+ + 4e^- \rightarrow HCHO + 2H_2O$	−0.213
$CO_3^{2-} + 8H^+ + 6e^- \rightarrow CH_3OH + 2H_2O$	−0.201
$CO_3^{2-} + 6H^+ + 4e^- \rightarrow C + 3H_2O$	0.065

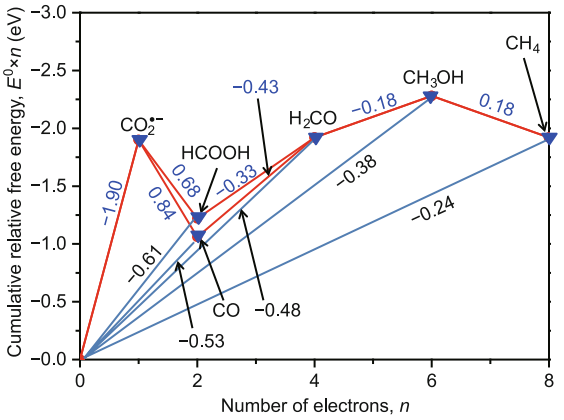

Figure 1 Latimer–Frost diagram for the multi-electron, multi-proton reduction of CO_2 in aqueous solution at pH 7.

step necessary for converting CO_2 to CO, then to H_2CO, then to hydrocarbons or alcohols also has low kinetic barriers [31,32]. Therefore, in comparison with the mono-electron process, proton-assisted multielectron transfer is an alternative and more favorable pathway to reduce CO_2.

H_2CO_3 and the carbonate ions in the solution can be reduced to a number of products, such as CH_3OH, HCOOH, and HCHO, through multi-electron transfer processes. The potentials calculated for H_2CO_3 and CO_3^{2-} are also listed in Table 1, respectively [28,29]. When comparing them, it is clear that the route of methanol formation from H_2CO_3 or CO_3^{2-} is more thermodynamically favorable than that from CO_2.

Because of high stability and low energy grade of CO_2, the chemical transformations of CO_2 are thermodynamically highly unfavorable. As a consequence, a large input of energy is required to drive the desired transformations. Moreover, the use of catalysts is necessary owing to its inertness [27,33]. Therefore, the reduction reaction of CO_2 is quite challenging. So far, thermochemical, electrochemical, photoelectrochemical (PEC), and photochemical reductions of CO_2 into hydrocarbon fuels with the help of catalysts have been extensively studied [33–35]. Without producing more CO_2, economical and environment-friendly reduction of CO_2 to value added chemicals is highly desired, which is possible only if renewable energy, such as solar energy, is used as the energy source. Among them, development of APS systems, such as PEC or photochemical reduction of CO_2 into solar fuel, is one of the ultimate goals in the reduction of CO_2 [36]. For example, in 1978, Halmann [6] first found that CO_2 was photoelectrochemically reduced to CH_3OH on a *p*-type GaP electrode. In the second year, Inoue *et al.* [5] first reported that formic acid, formaldehyde, and methyl alcohol could be produced through the photocatalytic reduction of CO_2 in aqueous suspensions of semiconductors such as TiO_2, ZnO, CdS, GaP and SiC. Through APS systems, solar energy and CO_2 are directly transformed and stored as chemical energy such as CH_3OH. Consequently, the photoreduction of CO_2 to solar fuel is particularly interesting and amazing, and has been extensively studied in the past decades.

It is well known that the photocatalytic properties of semiconductor mainly come from the formation of photogenerated charge carriers (holes and electrons) which occur upon the absorption of photons with energy equal to or greater than the band gap energy (E_g) separating the valence band (VB) from the conduction band (CB) (Fig. 2) [37,38]. The photogenerated holes in the VB diffuse to the semiconductor surface and react with water to produce O_2 or form hydroxyl radicals (•OH). Then, hydroxyl radicals further oxidize nearby organic molecules on the semicon-

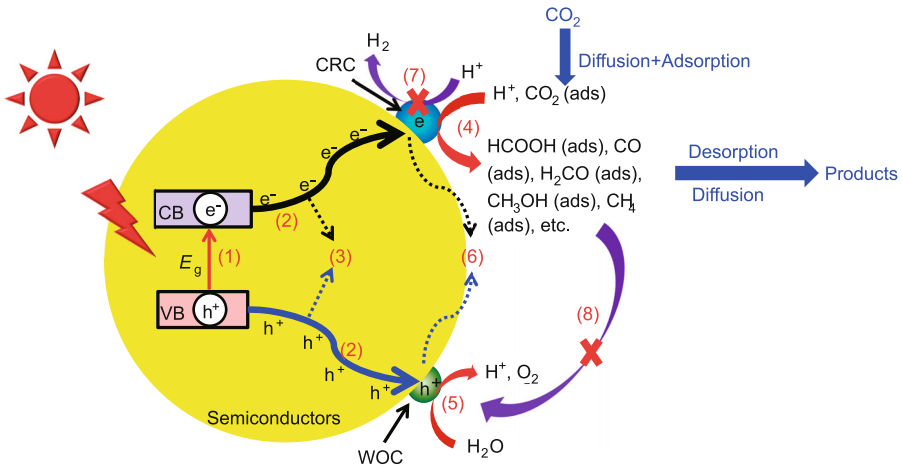

Figure 2 Processes involved in photocatalytic CO_2 reduction over a heterogeneous photocatalyst. CRC, CO_2 reduction co-catalysts; WOC, water oxidation co-catalysts.

ductor surface [37,38]. Meanwhile, electrons in the CB participate in reduction processes, which typically react with water to produce H_2 or with CO_2 to produce fuel [4,37,38]. To achieve CO_2 photoreduction, a good photocatalyst must have suitable band positions (VB and CB) and E_g. In other words, the bottoms of CB must be located at a more negative potential than the reduction potentials of CO_2, whereas the tops of the valence bands must be positioned more positively than the oxidation potential of H_2O to O_2, the redox reaction can proceed under irradiation at an energy equivalent to or greater than the band gap of the semiconductor photocatalyst [16]. Importantly, the yields of products from CO_2 reduction increase as the CB becomes more negative with respect to the redox potential of a certain reaction of CO_2 reduction, which has been demonstrated by the pioneering report in 1979 [5].

Based on this principle, it is easily found that many candidate materials with suitable CB positions are suitable for photocatalytic reduction of CO_2. Several potential semiconductors (e.g., TiO_2 [19,39], ZnO [5,40–43], ZnS [36,44–47], $SrTiO_3$ [11,48–50], SiC [5,51–53], Cu_2O [54–57], CdS [5,58–63], GaP [5,64], TaON [65–68], C_3N_4 [69–71], $BiVO_4$ [72–76] and Ta_3N_5 [77–80]) are listed in Fig. 3. Among them, TiO_2 is the most studied photocatalyst for CO_2 reduction because it is cheap, nontoxic, made up of abundant elements, and resistant to photocorrosion. However, its poor visible light absorption ability should be enhanced. Meanwhile, Cu_2O, CdS, GaP, TaON, C_3N_4 and Ta_3N_5 are good candidates for photocatalytic reduction of CO_2 under visible light irradiation. However, their weak photostability should be improved. The photocatalysts with more negative CB levels (in the right side of Fig. 3) seem to be better choices for the photocatalytic reduction of CO_2.

Process and mechanism of photocatalytic CO_2 reduction

Process of photocatalytic CO_2 reduction

In addition to suitable E_g and CB potentials, there are many other factors influencing the overall efficiency of photocatalytic CO_2 reduction, such as photocatalytic process and CO_2 reduction kinetics. Typical processes of photocatalytic CO_2 reduction over a semiconductor photocatalyst are illustrated in Fig. 2. They include the excitation, transport, separation, the elctrocatalytic reduction of CO_2 and water oxidation.

The first step (1) in Fig. 2 is the excitation of photo-generated electron-hole pairs in the bulk of semiconductor particles by absorbing photon energy greater than the band gap energy of a material. Therefore, to increase the excitation efficiency of electron-hole pairs by visible light, a photocatalyst should have a much narrower band gap (E_g < 3.0 eV or λ > 415 nm). From the viewpoint of visible light utilization, it should be an efficient strategy to develop visible-light-driven photocatalysts.

The second step (2) in Fig. 2 shows the separation of excited electrons and holes and their migration to the surface for the desired chemical reaction. As a competitive process, the bulk charge recombination, step (3), is an important deactivation process because the number of excited charge carriers significantly decreases by generating phonons or heat. To enhance the overall efficiency, it is of significant importance to improve transfer of photo-generated charge carriers to surface and inhibit their recombination in the bulk. Clearly, the structural and electronic properties of a photocatalyst have significant effects on these two steps. Thus, any strategy beneficial to the charge separation and transport, such as fabrication of nano-structured semicon-

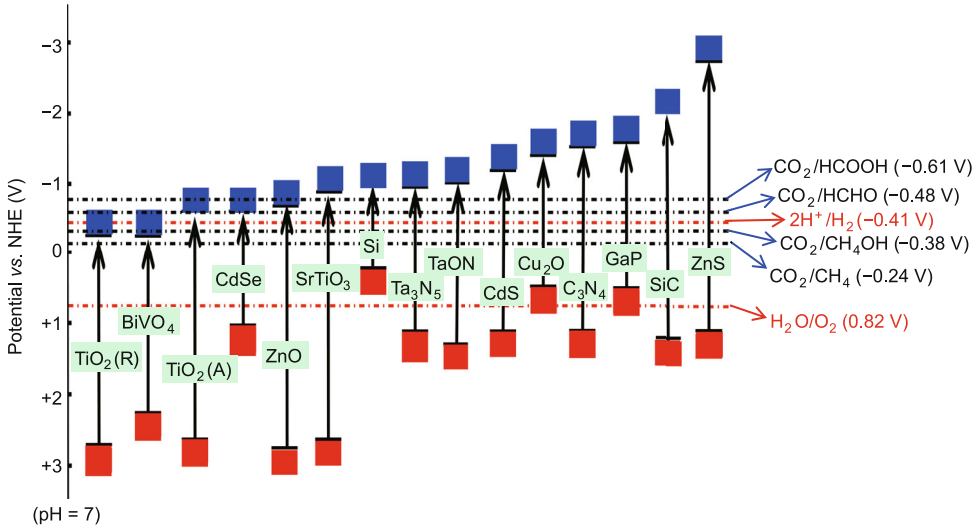

Figure 3 Band positions of some semiconductor photocatalysts and the redox potentials of CO_2 reduction at pH 7 in aqueous solution.

ductor, semiconductor heterojunctions or semiconductor/nano-carbon heterojunctions, should be taken into account to maximize the utilization rate of photo-generated charge carriers.

Once the photogenerated electrons reach the surface, the step (4) will occur. The process (4) is the electrocatalytic reduction of CO_2 by photo-generated electrons trapped in the CO_2 reduction co-catalysts (CRC) or the surface active sites. This process is usually a multi-electron and multi-step process involving a cascade of reactions, electron and proton transfer, C–O bond breaking, C–H/C-C bond formation and a multitude of products [81–86]. In most cases, the CRC should be loaded on the surface of semiconductors to achieve a highly efficient and selective reduction of CO_2 to specific products. During the photocatalytic reduction of CO_2, the formation of stable products requires at least two electrons, because some of products or intermediates are unstable or difficult to detect and quantify. Accordingly, the multistep mechanism is very complex. Any efficient strategy that promotes CO_2 reduction kinetics should be considered to be a possible way to boost the efficiency, such as developing mesoporous photocatalysts and loading CRC.

Meanwhile, the step (5) will also occur when the photogenerated holes reach the surface. The step (5) represents the electrocatalytic oxidation of water by the photogenerated holes trapped in the water oxidation co-catalysts (WOC) or the surface active sites. Improving water oxidation can promote the separation of photo-generated charge carriers on the surface of semiconductors, thus leading to the enhancement in activity for CO_2 photoreduction. In addition, the process (6), surface charge recombination, will occur if there are no enough active sites or co-catalysts on the surface of semiconductors. Apparently, the surface charge recombination should also be avoided because it is also ineffective for photocatalytic CO_2 reduction process, whereas the surface trapping should be enhanced by improving surface properties of the photocatalysts such as surface reaction sites, surface states and morphology.

In addition, the processes (7) and (8) in Fig. 2 represent the electrocatalytic H_2 evolution by trapped photo-generated electrons in CO_2 reduction co-catalysts and the electrocatalytic oxidation of reduction products by water oxidation co-catalysts, respectively. In the processes (7), the H_2 evolution will greatly decrease the utilization rates of photo-generated electrons for CO_2 reduction. In the processes (8), the oxidation of CO_2 reduction products by photo-generated holes is harmful for both water oxidation and CO_2 reduction. Clearly, these two processes are the unfavorable ones, because they could significantly reduce the quantum yield of photocatalysts for CO_2 photoreduction. Thus, to design highly efficient photocatalysts for photocatalytic CO_2 reduction, these factors should be comprehensively considered and the effective strategies should also be developed to avoid or decrease these unfavorable processes.

Mechanism and kinetics of photocatalytic CO_2 reduction

One famous mechanism based on the formation of CO_2^- radical anion was first suggested by Anpo *et al.* [86]. In terms of this mechanism, the adsorbed CO_2 molecule was activated by a one-electron reduction, leading to the formation of surface-bound CO_2^- radical anion. Then, the CO_2^- radical anion was selectively reduced to CO (or HCOOH), CH_2OH, CH_3OH and CH_4 by the photo-generated electrons, H^+, hydrogen radical ($H^\bullet$) and OH radical ($OH^\bullet$) [5,17,83–85]. Although the COO_2^- radicals and CO_2 reduction intermediates during the processes of CO_2 reduction have been identified by different spectroscopy [86–88], the one-electron reduction of CO_2 is thermodynamically unfavorable due to the highly negative electrochemical reduction potential (−1.9 V *vs.* NHE) of the anion radical CO_2^- and the low CB potential of semiconductors. Therefore, most favorable reaction pathways consisting of a multiple electron transfer have been also reported.

The two-electron, two-proton reaction pathway is one typical multiple-electron reaction mechanism, which was first proposed by Inoue and co-workers [5] based on small amounts of formic acid, formaldehyde, methyl alcohol, and methane produced by photoreduction of CO_2. A multi-step reduction process of conversion of CO_2 to methane can be described using Equation (7).

$$CO_2 \xrightarrow[+2H^+]{+2e^-} HCO_2H \xrightarrow[+2H^+ -H_2O]{+2e^-} H_2CO \xrightarrow[+2H^+]{+2e^-} CH_3OH \xrightarrow[+2H^+ -H_2O]{+2e^-} CH_4, \quad (7)$$

$$CO_2 + 2e^- + H^+ \rightarrow HCOO^-. \quad (8)$$

A similar route involving surface formate species as the primary intermediate has been also proposed by Wu *et al.* [89] on the basis of *in-situ* IR spectroscopic studies. The bicarbonate, carbonate, formate, formaldehyde and methoxy species on TiO_2 surface were observed from IR absorption bands. A concerted two-electron and one-proton transfer (see Equation (8)) to adsorbed CO_2 molecules on the TiO_2 surface was also demonstrated by Dimitrijevic *et al.* [90] using low temperature electron paramagnetic resonance (EPR) measurements. The formation of H atoms and $OH^\bullet$ radicals in addition to methyl ($^\bullet CH_3$) and methoxy ($^\bullet CH_3O$) radicals on the surface was also observed by the electron spin resonance (ESR) results. Then the reaction of methoxyl radical with H_2O can lead to the formation of methanol. However, it appears clearly that methanol or formic acid as intermediates in the formation of hydrocarbons on Ti-SBA-15 is impossible because added methanol or formic

acid does not enhance the concentration of hydrocarbons. While, added formaldehyde can increase the photoconversion of CO_2 to hydrocarbon products [91]. Meanwhile, Frei and coworkers [92,93] demonstrated that formic acid is the primary 2-electron reduction product of CO_2 at the excited Ti centers of Ti silicalite molecular sieve using methanol as electron donor, while CO is the single-photon, 2-electron-transfer reduction product of CO_2 at framework Ti centers with H_2O acting as an electron donor. Moreover, methyl formate was also mainly produced for photocatalytic reduction of CO_2 over some other photocatalysts (such as Bi_2S_3 [94], CuO-TiO_2 [95], Ni-doped ZnS [96] and Ag Loaded $SrTiO_3$ [49]) in methanol solution. Therefore, the two-electron, two-proton reaction steps from methanol or formic acid to hydrocarbons on most semiconductors seem to be impossible in many systems.

A hypothesis, the CO would react with atomic hydrogen to form hydrocarbons, was also proposed by Varghese *et al.* [97]. The possible reactions are seen in Equation (9–14):

$$H_2O + 2h^+ \rightarrow 1/2O_2 + 2H^+, \quad (9)$$

$$H_2O + h^+ \rightarrow {}^{\bullet}OH + H^+, \quad (10)$$

$$H^+ + e^- \rightarrow H^{\bullet}, \quad (11)$$

$$H^{\bullet} + H^{\bullet} \rightarrow H_2, \quad (12)$$

$$2CO_2 + 4e^- \rightarrow 2CO + O_2, \quad (13)$$

$$CO + 6e^- + 6H^+ \rightarrow CH_4 + H_2O. \quad (14)$$

However, the validity of this hypothesis need to be further verified. Meanwhile, another reaction mechanism through the formation of CO in the initial stages followed by its conversion to formaldehyde, then to other hydrocarbon products was proposed by Yang *et al.* [91]. Importantly, it also showed that formaldehyde is extremely reactive over Ti-SBA-15 and that the formation of C_2 and $>C_2$ hydrocarbons could be also explained through this mechanism.

Recently, a mechanism involving dimerization of surface C_1 species was proposed as a possible route for the formation of C_2 hydrocarbon products [98,99]. Interestingly, Shkrob *et al.* [87] recently reported a glyoxal cycle for CO_2 fixation. In addition to methane, this cycle generates complicated organic molecules, such as glycolaldehyde, acetaldehyde, and methylformate, which were observed in product analyses. This cycle can be regarded as one of the simplest realizations of multistep, photosynthetic fixation of atmospheric carbon in prebiotic nature [87]. Therefore, the glyoxal cycle accounts for several known byproducts, such as methanol, formate, formaldehyde, acetaldehyde, and methylformate, which provides a new idea to study the mechanisms for photocatalytic reduction of CO_2. Thus, it is clear that the products for CO_2 photoreduction in aqueous medium exist in both the gas and liquid phases. However, most researchers only measured one or two of reduction products in liquid phase and ignored the analysis of products in gas phase, which was not beneficial for a detailed study on the mechanism of CO_2 photoreduction and the selectivity of products. Therefore, in addition to the measurements of products in liquid phase, it is also important to analyze the reduction products in the gas for CO_2 photoreduction in aqueous medium [83,100,101]. Special attention should also be focused on the photocatalytic reduction of CO_2 to C_x ($x \geqslant 2$) organic compounds, which is also promising and has received far less attention than analogous systems leading to C_1 products [84,98,99].

Furthermore, the kinetic equations based on different mechanisms were developed for modeling the photocatalytic reduction of CO_2. A Langmuir–Hinshelwood type kinetic equation was first developed for modeling the photocatalytic reduction of carbonate by the UV/TiO_2 process in aqueous solution [102]. The results indicate that the photocatalytic reduction rate of carbonate is adsorption-controlled [102]. Meanwhile, a one-site Langmuir–Hinshewood (L–H) kinetic model was further applied to simulate the photoreduction rate of CO_2 to CO (or H_2) and CH_4 using H_2O over TiO_2 [102–105]. In addition, Anpo's mechanism, wherein CO is proposed as the primary intermediate, was well supported by this kinetic model [102–104].

In summary, the complex photocatalytic processes and kinetics of CO_2 reduction on semiconductors lead to a very low efficiency of CO_2 photoreduction. It is clear that the reduction potentials of CO_2 to CH_3OH and CH_4 products are thermodynamically more feasible than that required to reduce protons to H_2. However, the kinetics of CO_2 reduction is unfavorable due to the multi-electron reduction processes. At this point, the kinetic challenges are great, and thus the improvements of kinetics of CO_2 reduction play important roles in enhancing the overall efficiency. Meanwhile, the complex photocatalytic processes, including excitation, transport, separation, adsorption and activation of CO_2, CO_2 reduction kinetics and water oxidation have also important impacts on the overall efficiency of CO_2 reduction. Therefore, the control of photocatalytic processes and kinetics of CO_2 reduction is rather critical to enhance the overall efficiency, which is strongly dependent on the bulk and surface properties of photocatalysts and can be improved by rational design and fabrication of photocatalysts [16,106,107].

All factors influencing the efficiency of photocatalytic CO_2 reduction, including charge excitation and transport, adsorption and activation of CO_2, CO_2 reduction kinetics and undesirable reaction are summarized in Fig. 4. As shown in Fig. 4, to achieve a high efficiency and selectivity, the corresponding engineering strategies including increased visible-light excitation, improved charge transfer and separation, enhanced adsorption and activation of

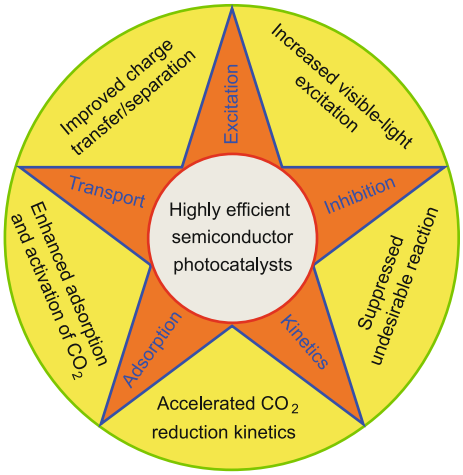

Figure 4 Factors influencing photocatalytic efficiency and corresponding design strategies for highly efficient photocatalysts used in the photocatalytic reduction of CO_2.

CO_2, accelerated CO_2 reduction kinetics and suppressed undesirable reaction, can be used to manage photo-generated charges and enhance the overall efficiency, which will be discussed in detail in the following sections.

STRATEGIES FOR DESIGN AND FABRICATION OF PHOTOCATALYSTS FOR CO_2 REDUCTION

Increased visible-light excitation

As described above, the process (1) in Fig. 2 is strongly dependent on the band gap of a semiconductor photocatalyst. The low visible light absorption is a key factor affecting the photocatalytic efficiency of many wide band gap semiconductors. This is because the wide band gap makes semiconductors active only in ultraviolet region of the solar spectrum (about a 4% of the total sunlight energy), and limits utilization of light in visible region (about 48% of the total sunlight energy). Therefore, many efforts have been made to search for the visible-light-driven photocatalysts. One typical strategy is to exploit new single-phase visible-light-driven photocatalysts (e.g., CdS [60,63,108], C_3N_4 [69,109,110], WO_3 [111,112], $CaFe_2O_4$ [113,114], $LaCoO_3$ [115], $BiVO_4$ [116,117], Bi_2WO_4 [118,119], $Fe_2V_4O_{13}$ [120] and $InTaO_4$ [121–124]), which have proven to be active for photocatalytic reduction of CO_2 in visible region. The other typical strategy is to make the wide band gap semiconductors active in visible region through a suitable modification. As shown in Fig. 5, there are generally five strategies to develop visible-light-driven photocatalysts from wide band gap semiconductors: impurity doping, introduction of structural defects, sensitization, surface plasmon resonance (SPR) effect and solid solution, all of which have been applied in the fields of photocatalytic reduction of CO_2.

Impurity doping

The first strategy is to tune the electronic properties and visible-light response of semiconductor nanocrystals via an impurity doping, which can introduce a localized electronic states (LS) into the band gap of a wide band gap semiconductor, thus achieving a two-step photoexcitation by the low-energy visible-light photons [125]. On the one hand, nonmetal ion doping such as nitrogen and iodine can lead to an obvious red shift in optical response and an significant enhancement in the visible light activity of wide band gap semiconductors, although there is still a lively debates about the causes for red-shifts of the absorption edges [126]. For example, Li *et al.* [127] reported that nitrogen-doped mesoporous TiO_2 samples displayed good visible-light absorption and enhanced activity for CO_2 photoreduction to methane by water in gas phase under visible-light irradiation. It was believed that the mesoporous structure and N-doping were responsible for inhibiting the recombination of photogenerated electrons and holes and improving visible light absorption, respectively, thus leading to an improved photoactivity. The mesoporous nitrogen doped Ta_2O_5 exhibits excellent photocatalytic activity for hydrogen evolution and CO_2 reduction (modified with ruthenium-complex) under visible-light irradiation due to their larger surface area, enhanced visible light absorption and controlled morphology [128]. Similar results were observed for nitrogen-doped $InTaO_4$ photocatalysts, which showed a 2-fold increase in the yield of methanol compared to the undoped one [124]. In addition to N-doped TiO_2, iodine-doped TiO_2 (I-TiO_2) nanoporticles (NPs) demonstrated significant enhancements in

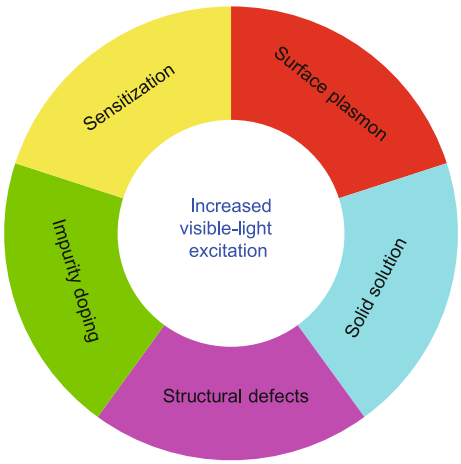

Figure 5 Typical strategies for increasing visible-light excitation.

CO_2 photoreduction to CO compared with undoped TiO_2 under both visible and UV-vis irradiations. The possible reasons are the synergistic effects of slightly increased surface area, enhanced visible light absorption, and improved charge separation owing to the iodine doping [129]. The further enhancements in CO_2 photoreduction to CO were also achieved by copper and iodine co-modified TiO_2 NPs (Cu-I-TiO_2) [130].

On the other hand, metal ion doping can also create the impurity levels in the forbidden band of wide-band gap semiconductors, which can also enhance their absorption for visible light. Furthermore, the doped metal ion can also perform as electron traps and active sites for highly selective CO_2 photoreduction. It is well known that TiO_2 doped with copper shows good selectivity for CH_3OH from the reduction of CO_2, which will be discussed below [55,131–133]. Besides Cu, other metal-ion doping such as Ce [134], Mn [135], Ru [83,136], Ni [96,137], In [105], Fe [89], Ag [89,132], Au [136,138], Mg [139] and their co-doping with Cu or N have also been reported for photocatalytic reduction of CO_2 and exhibit enhanced photocatalytic activities for the reduction of CO_2. Generally, a metal cation doping of TiO_2 not only creates oxygen vacancies and new active sites for the reaction, but also introduces localized mid-gap states which contribute to charge separation and the absorption of visible light [39]. In addition, self-doped Ti^{3+} is also an effective strategy to enhance the photocatalytic activity of TiO_2 under visible light, which deserves more attention in photocatalytic reduction of CO_2 [140]. It should be noted that the excess amount of dopants as recombination centers can also lead to a greatly decreased activity for CO_2 photoreduction. Thus, it is rather important to optimize dopant concentration to achieve the highest activity for CO_2 photoreduction.

Introduction of structural defects

The second effective strategy to enhance the visible light activity of wide band gap photocatalysts is to introduce defects (such as oxygen vacancies) on the surface of semiconductor substrates, which can effectively tailor their electronic structure, thus leading to an enhanced visible light absorption, improved charge transport and separation and increased active sites for adsorption and reduction of CO_2 [141,142]. The previous results showed that the oxygen vacancies on the surface of semiconductors play important roles in the photocatalytic reduction of CO_2 under visible light. Liu *et al.* [143] first systematically studied the photoreduction of CO_2 with H_2O on defect-free and defective TiO_2 anatase, rutile, and brookite nanocrystals, respectively. It was found that the activity of the defective brookite (He-pretreated samples) was enhanced by a factor of 10.3 for CO production and 8.2 for CH_4 production. The photocatalytic activities for CO_2 reduction over un-pretreated samples follow the order anatase > brookite > rutile. The enhancement in the production of CO and CH_4 from CO_2 photoreduction was primarily attributed to the creation of oxygen vacancies and Ti^{3+} on the surface [143]. A H_2-pretreated Cu/TiO_2 exhibited a 10-fold and 189-fold enhancement in the photoreduction of CO_2 to CO and CH_4, respectively [144]. The existence of Cu^+/Cu^0 couples and the formation of surface defect sites (such as oxygen vacancies and Ti^{3+}) in the H_2-pretreated Cu/TiO_2 can greatly improve CO_2 adsorption, charge transfer and trapping at the active sites of the adsorbed CO_2, thus leading to the significant enhancement in the activity for CO_2 production [144]. The existence of oxide vacancies on the surface of $Bi_6Mo_2O_{15}$ sub-microwires enhanced the photocatalytic activity toward the photoreduction of CO_2 into CH_4 through capturing photo-generated electrons at the surface [145]. Recently, it was also reported that a highly selective photoreduction of CO_2 to CO was achieved over defective CeO_2 nanorods under ambient conditions (CO_2, 400 ppm) due to the synergistic effects of local strain and surface oxygen vacancies [146]. More interestingly, the ultrathin $W_{18}O_{49}$ nanowires with diameters below 1 nm also exhibited very high activity for CO_2 photoreduction to methane which was several hundred times higher than that of commercial WO_3 due to the presence of a large number of oxygen vacancies [141].

Similar results were obtained in the metal sulfide semiconductors. The quantized ZnS crystallites with low density of surface defects are indispensable for effective CO_2 reduction owing to stabilization of the electron-hole pair against recombination and elimination of electron deactivation by surface traps [36]. The surface sulfur vacancies on CdS-DMF surface formed by reaction with the excess Cd^{2+} added in the systems can act as adsorptive sites for the CO_2 molecule and increase the photocatalytic activity for reduction of CO_2 to CO [58]. Meanwhile, the surface sulfur vacancies on the surface of ZnS-DMF(ClO_4) formed by addition of excess Zn^{2+} result in the change in the product distribution without losing photocatalytic activity [46].

In addition, the location of defects and the relative concentration ratio of bulk defects to surface defects in photocatalysts have also profound effects on their electronic properties and photocatalytic activities [147,148]. Therefore, the density and location of defects should be paid more attention for the application of CO_2 photoreduction in future studies.

Sensitization

The third effective strategy is to sensitize wide band gap semiconductors using dye and quantum dots (QDs) with visible-light activity. Clearly, the sensitizers as the absorb-

ing species not only improve the sunlight harvesting due to their low band gap, but also inhibit the electron–hole recombination owing to the efficient charge separation by the semiconductor/sensitizer interface. Recently, dye-sensitized TiO_2 has also been reported in the photoreduction of CO_2 to fuels with H_2O. The formation rate of formic acid, methanol and formaldehyde on zinc-phthalocyanine (ZnPc) or CoPc sensitized TiO_2 are much higher than those of TiO_2 and physically absorbed CoPc(or ZnPc)/TiO_2 [149–151]. Recently, it was found that the graphene oxide (GO)-immobilized CoPc photocatalyst exhibited higher photocatalytic activity and selectivity for the photocatalytic reduction of CO_2 to methanol by using water as a solvent and triethylamine as the sacrificial donor. Importantly, the photocatalyst also showed good photostability during the reaction [152]. A new copper(I) dye-sensitized TiO_2^- based photocatalyst exhibits impressive effectiveness for the selective photoreduction of CO_2 to CH_4 under visible light [153]. Furthermore, full absorption of visible light of N_3-dye along with efficient charge transfer in N_3 dye-TiO_2 system gives rise to the superior photoreduction of the resulting dye-adsorbed catalyst [154]. However, the improvement of efficiency and long-term stability of dye-sensitized photocatalysts is still a great challenge for their practical applications. Meanwhile, a series of CdSe QD-sensitized Pt/TiO_2 hetero-structures yield 48 ppm g^{-1} h^{-1} of CH_4 and 3.3 ppm g^{-1} h^{-1} of CH_3OH (vapor) for photocatalytic reduction of CO_2 in the presence of H_2O under visible light irradiation ($\lambda > 420$ nm) [155]. The PbS QDs enhance CO_2 photoreduction rates over TiO_2 by a factor of 5 in comparison with un-sensitized photocatalysts under broad band illumination (UV-NIR) [156]. The activity of CdS (or Bi_2S_3) QD-sensitized TiO_2 nanotubes for photocatalytic reduction of CO_2 to CH_3OH was about 1.6 (or 2.2) times higher than that of TiO_2 nanotubes due to enhanced visible-light absorption and improved charge separation [63]. It was also reported that 23.2% AgBr sensitized TiO_2 exhibited relatively high activity and selectivity for methane and methanol production under visible light irradiation. The highly efficient photocatalytic activity of AgBr/TiO_2 is attributed to its strong absorption in the visible-light region and the improved transfer and separation of photo-excited electrons and holes [157]. Moreover, a new composite photocatalyst based on overlapping energy states of TiO_2 and copper indium sulfide (CIS) QDs was exploited, exhibiting the highest selectivity for ethane (> 70%) and a higher efficiency of converting ultraviolet radiation into fuels (4.3%) using concentrated sunlight (> 4 Sun illumination) [158]. In addition, a new class of green QDs, silicon and carbon QDs [159–162], were expected to apply in designing the QD-sensitized photocatalysts for photocatalytic reduction of CO_2.

Surface plasmon resonance (SPR) effect

The forth effective strategy is to use the localized surface plasmon resonance (SPR) effect, which refers to the collective oscillation of the conduction electrons in noble metal NPs (i.e., Au and Ag) under visible light irradiation [163]. Thus, the plasmonic noble metal NPS can serve as an alternative type of sensitizer to enhance the visible-light absorption of photocatalysts due to SPR effects. In recent years, the interesting SPR effects have also been reported in the photoreduction of CO_2 under visible light irradiation [138,164,165]. For instance, Zhang *et al.* [164] reported that the co-decoration of Au and Pt NPs with sizes of 5–12 nm on TiO_2 nanofibers could remarkably enhance their photocatalytic activity and selectivity for CO_2 reduction to CH_4. It was believed that the synergy of surface electron trapping of Pt and SPR of Au NPs greatly improve the charge separation of photoexcited TiO_2 (as illustrated in Fig. 6), thus leading to a significant enhancement in the activity of photocatalytic CO_2 reduction [164]. A 24-fold enhancement in activity and selectivity for photoreduction of CO_2 to CH_4 with water vapor was also observed because of the intense local electromagnetic fields created by the surface plasmons of Au NPs on TiO_2 [138].

Besides good selectivity of plasmonic Au for CH_4 production, the plasmonic Ag NPs have also attracted much attention due to their excellent selectivity for methanol in liquid phase system. The methanol yields of CO_2 photoreduction over the plasmonic-shaped AgCl:Ag and AgBr:Ag are 188.68 and 108.696 μmol g^{-1}, under visible-light irradiation, respectively, due to the SPR of Ag NPs [166]. The 2.5% Ag/TiO_2 exhibited the best activity for photocatalytic reduction of CO_2 to methanol due to the SPR effects, which was 9.4 times higher than that of pure TiO_2 [167]. Furthermore, the CH_4 yield over plasmonic Ag NPs/TiO_2 nanorods was almost 5 times higher than that of undecorated

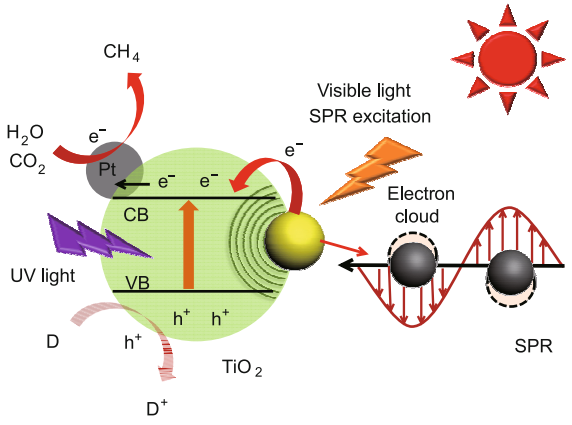

Figure 6 Schematic diagram of photocatalytic process for CO_2 reduction on the Au/Pt/TiO_2 nanofibers.

TiO_2 nanorods in gas phase system, which was correlated with the SPR effect and structure of TiO_2 nanorods [168].

In addition, it was reported that the Cu-TiO_2 nanorod films showed about twice the rate observed with pure titania films due to better separation of photogenerated electrons and holes and mild SPR effects [169]. Since Au and Ag are noble metals, in future studies, more attention should be placed on plasmonic Cu NPs or alloy plasmonic NPs with better selectivity for CO_2 reduction [170–173].

Solid solution

The fifth effective strategy is solid solution, which can be formed through adding a narrow band gap semiconductor (for example, Ag_2O, Cu_2O, Fe_2O_3, Cr_2O_3, CuO and so on) into a wide band gap semiconductor. Both the band gap and position can be continuously adjusted by varying the ratio of the compositions of the narrow and the wide band gap semiconductors in the solid solution. Thus, the electronic structures and the photocatalytic performances of a semiconductor can be efficiently optimized. Recently, many researchers have revealed that solid solutions exhibited relatively high activity and selectivity for photocatalytic reduction CO_2 to methanol, methane or ethanol under visible light. The multicomponent metal oxides (e.g., $CuGa_{1-x}Fe_xO_2$ [174]), metal sulfides (e.g., solid solutions of ZnS-CdS microcrystals [45] and $Cu_xAg_yIn_zZn_kS_m$ [175]) and oxynitrides (e.g., zinc germanium oxynitride [176]) exhibited high activity for the photoreduction of CO_2 under visible light irradiation. For instance, the yellow $Zn_{1.7}GeN_{1.8}O$ solid solution, synthesized by the nitridation of the wide-band-gap Zn_2GeO_4, exhibits high activity for photocatalytic reduction CO_2 into CH_4 with H_2O at room temperature under visible light irradiation. The reported photonic yield for $Zn_{1.7}GeN_{1.8}O$ at 420 nm was 0.024% [177]. The further research showed that CH_4 evolution over mesoporous zinc germanium oxynitride nitrided over a 10-h period is about 26.8 ppm g^{-1}, which is even higher than that of commercial nitrogen-doped TiO_2 (22.1 ppm g^{-1}) under visible light [176]. The $(Ga_{1-x}Zn_x)(N_{1-x}O_x)$ solid solutions with a band gap of 2.2–2.7 eV exhibited a high visible-light activity for photocatalytic conversion of CO_2 and H_2O into hydrocarbon fuel [178]. A high activity in converting CO_2 and H_2O into CH_4 and O_2 was achieved over zinc gallogermanate solid solution synthesized by introducing Zn_2GeO_4 into $ZnGa_2O_4$, due to improved hole mobility, enhanced water oxidation ability and effectively narrowed band gap [179]. Importantly, this zinc gallogermanate solid was prepared by a hydrothermal ion exchange reaction, which is beneficial to its surface area enhancement.

So far, most of these oxides are synthesized by high temperature solid state reaction with very low surface area. The preparation of high surface area photocatalysts with mesoporous structures is still a great challenge. Thus, to further boost the photocatalytic activities, it is highly desired to prepare mesoporous photocatalysts with high crystallinity by soft chemistry routes.

Promoted charge transfer/separation

As mentioned above, the process (3) and (6) account for the bulk and surface recombination of photo-generated electron-hole pairs, respectively. Obviously, the above two processes are detrimental to photocatalytic efficiency enhancement of a semiconductor photocatalyst due to the decreased utilization rate of carriers for desired photoreactions. Meanwhile, the process (2) represents the charge transfer to the surface without recombination, which is dependent on the crystal structure, crystallinity and particle size of a semiconductor photocatalyst. Thus, the issue of photo-generated charge transfer and separation has become another key factor strongly affecting the efficiency of photocatalysis process. So far, a number of strategies have been employed to promote the transfer and separation of the photo-induced electrons and holes. Here, three dominant strategies including nanostructured photocatalysts, semiconductor heterojunctions and semiconductor/nano-carbon heterojunctions will be discussed in detail.

Nanostructured photocatalysts

An efficient strategy for accelerating the transfer and separation of the photo-induced carriers is to construct nanostructured photocatalysts. As is known, the nano-architectures (e.g., physical dimensions, sizes, shapes and porous structures) of semiconductors have profound impacts on their photocatalytic performances. Generally, semiconductor nanomaterials have several advantages over their bulk counterparts for solar fuel generation due to the following reasons: higher surface-to-volume ratio, higher optical absorption, shorter charge migration length, stronger redox power and tunable electronic structure [180]. Furthermore, the photo-generated charges can also be efficiently separated to avoid bulk/surface charge recombination and transfer to the separated active sites on the surface of the photocatalysts. The relevant nanostructures including 0D nanocrystals, 1D nanowires/rods, 2D nanosheets and 3D hierarchical architectures have been widely investigated, which will also be discussed in detail in this section.

First, the construction of 0D nanocrystal photocatalysts has also become a widely accepted strategy to enhance the photocatalytic activities for CO_2 reduction because of the nanosized and quantum size effects. Kocí *et al.* [100] studied the photoreduction of CO_2 by water upon pure TiO_2 anatase particles with a crystallite diameters ranging from 4.5 to 29 nm. Methane and methanol were the main reduction products. The optimum particle size correspond-

ing to the highest yields of both products was 14 nm. The observed optimum particle size is a result of competing effects of specific surface area, charge-carrier dynamics and light absorption efficiency [100]. Liu *et al.* [181] studied the photocatalytic reduction of CO_2 in various kinds of solvents using TiO_2 nanocrystals embedded in SiO_2 (Q-TiO_2/SiO_2) with an average diameter of 5.3 nm. Apart from TiO_2 [143,181–183], other semiconductor NPs such as ZnS [36,46], CdS [62,184] and silicon [185] nanocrystals have also been found to exhibit better photocatalytic activities for the reduction of CO_2. Consequently, with regard to the application of nanocrystalline semiconductors, it is important to obtain the optimal particle size for maximizing their photocatalytic efficiency for CO_2 photoreduction. In addition, to prevent agglomeration of these particles, they should be capped with polymers or anchored on a stable support [2].

Second, there are many reports about the application of 1D nanostructures in photocatalytic reduction of CO_2 due to the shortened distance for charges to diffuse to the semiconductor/electrolyte interface and improved transport properties of charge carriers. TiO_2 nanotubes [63,97,186–191], nanofibers [192] and nanorods [168,169,193] exhibited a much better photocatalytic activity for CO_2 reduction than P25 or TiO_2 NPs. For instance, Fu *et al.* [192] demonstrated that the TiO_2 nanofibers with a 2-h solvothermal treatment exhibited the highest activity for photocatalytic reduction of CO_2 to CH_4, which was about 6 and 25 times higher than those of TiO_2 nanofibers without solvothermal treatment and P25, respectively, due to the enhanced CO_2 adsorption capacity and the improved charge separation. Moreover, $NaNbO_3$ nanowires [194], Zn_2GeO_4 nanoribbons [195] and nanorods [196] synthesized using a hydrothermal/solvothermal route showed much better photocatalytic activity for the conversion of CO_2 to CO or CH_4 than the corresponding samples prepared by a high-temperature solid state reaction. In addition, the surface area value and the activity of HNb_3O_8 nanobelts prepared by hydrothermal synthesis increased six and twenty times, respectively, in comparison with those of HNb_3O_8 particles prepared by solid state reaction [197].

Third, there is an increasing interest in developing 2D nanosheet-based semiconductors with dominant high-energy facets for the application in photocatalytic reduction of CO_2 because of their facet-dependent properties. Among them, TiO_2 nanosheets with exposed (100), (010), (101) or (001) facets were the most widely investigated photocatalysts in this field [172,198–201]. For instance, the anatase TiO_2 ultrathin nanosheets with 95% exposed (100) facets showed a 5 times higher photocatalytic activity for reduction of CO_2 to CH_4 than TiO_2 cuboids with 53% exposed (100) facets [198]. The anatase TiO_2 single crystals and mesocrystals with dominant (101) facets exhibited a much superior activity towards CH_4 generation from photoreduction of CO_2, in comparison with solid crystals [199]. The anatase TiO_2 (010) facets demonstrated a higher photocatalytic reduction efficiency of CO_2 to CH_4 than (001) facets due to its larger CO_2 adsorbed amount and longer charge lifetime [200]. More interestingly, Yu and coworkers [201] reported that the highest activity of TiO_2 nanosheet for photoreduction of CO_2 to CH_4 can be achieved at an optimal ratio of the exposed (101) and (001) facets (45 : 55). This is attributed to the synergistic effect of an electron overflow and surface heterojunction between the co-exposed (101) and (001) facets of anatase (Fig. 7). Importantly, the concept of surface heterojunction was first proposed in terms of the density functional theory (DFT) calculations, which may provide a new strategy for designing sufficiently efficient photocatalysts [201].

In addition, $ZnGa_2O_4$ nanocube with the exposed (100) or (110) facets [202,203], Bi_2WO_6 square nanoplates with the exposed (001) surface [118], BiOCl nanoplates with oxygen vacancies [204], nanoplate-textured Zn_2SnO_4 with the exposed (100) surface [205] and WO_3 nanosheets with

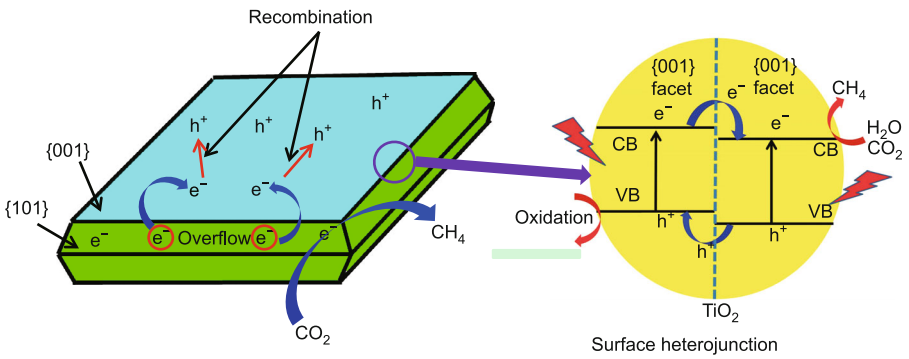

Figure 7 An overflow effect and hetero-facet junction between (101) and (001) facets in anatase.

the exposed (001) surface [111] were successively reported. These nanoplate/nanosheet photocatalysts exhibit enhanced performance for photocatalytic reduction of CO_2 into CH_4 in the presence of water vapor due to the improved separation of photo-generated electron and hole pairs. However, so far, the photocatalytic selectivity on different facets of various semiconductors has not been studied systemically for the photoreduction of CO_2. Thus, it is still very interesting to identify optimal ratio and the selectivity of different facets for CO_2 photoreduction. In addition, much attention should be also paid to the simple and efficient methods to prepare nanosheets such as liquid exfoliation of layered materials [206].

Finally, it is known that 3D hierarchical semiconductor architectures assembled by nanoscaled building blocks generally display unique properties (such as the optical, electronic, and photocatalytic performances), which are distinguished from those of the mono-morphological structures. Thus, the 3D hierarchical semiconductor architectures have been widely applied in the CO_2 photoreduction due to their increased specific areas and adsorption of CO_2, as well as improved light harvesting and interfacial charge separation [94,119,207]. For example, Bi_2WO_6 hierarchical microspheres with hollow interiors synthesized via a facile anion exchange method display an excellent photoactivity for reduction of CO_2 to methanol (32.6 μmol g^{-1}), which is 25.5 times higher than that of Bi_2WO_6 prepared by solid state reaction (1.28 μmol g^{-1}) under the same conditions [119]. The significantly enhanced activity can be attributed to the improved surface area and high CO_2 adsorption capacity. Bi_2S_3 microspheres also showed the higher activity for photocatalytic reduction of CO_2 to methyl formate in methanol due to their special hierarchical structure, good permeability and high light-harvesting capacity, as compared with Bi_2S_3 NPs [94].

Semiconductor heterojunctions

Coupling semiconductors has also turned out to be another effective design strategy for improving their photocatalytic activity because better photo-generated charge transfer and separation can be achieved in the interface region between two different phases (or semiconductors) in close contact. In coupled semiconductors, the electric-field-assisted charge transport from one particle to the other via interfaces between the semiconductors with matching band potentials can be achieved, which can greatly improve the electron-hole separation, increase the lifetime of the charge carrier, and enhance the interfacial charge transfer efficiency to adsorbed substrate. Constructing heterophase junctions (homojunctions) and heterojunctions are two main strategies used in designing the coupled photocatalysts.

So far, TiO_2-based heterophase junction has been well developed in the photocatalytic reduction of CO_2. The bicrystalline anatase–brookite composite displays the strongest absorption in the visible–light region and on which the highest CH_3OH yield from CO_2 photoreduction is 3.4 times higher than that on P25 or anatase catalyst in an aqueous system due to its unique electrical band structures and efficient transfer of electrons from brookite to anatase [208]. Similarly, the bicrystalline mixture with a composition of 75% anatase and 25% brookite also showed the highest photocatalytic activity for CO_2 photoreduction to CO and CH_4 in the presence of water vapor, as compared with pure anatase, brookite, and P25 [209]. The rutile TiO_2 nanoparticle modified anatase TiO_2 nanorods showed high photocatalytic activity for CO_2 reduction to CH_4, which was almost two times higher than that of pure anatase TiO_2 nanorods [193]. A sputtered mixed-phase film (70% anatase, 30% rutile) deposited at low angle exhibited a strong red shift and the highest methane yield from the photoreduction of CO_2 compared to TiO_2 fabricated under other sputtering conditions and commercial standard Degussa P25 under UV irradiation [210]. Li *et al.* [211] modified the commercial anatase TiO_2 with the rutile by a low-temperature hydrothermal method and found that mixed-phase TiO_2 nanocomposites sintered in air at 773 K exhibited a much greater rate of methane formation than Degussa P25. In addition, compared with cubic and orthorhombic $NaNbO_3$, the activity of mixed-phase $NaNbO_3$ is enhanced by 30% and 200% in reducing CO_2 into CH_4, respectively, due to improved the charge separation by surface-junctions (Fig. 8) [212].

Since the wide band gap of TiO_2-based heterophase junctions limits their practical applications under visible light irradiation, the design of visible-light-driven photocatalysts with heterophase junctions has attracted much attention in recent years. Many visible-light-driven homojunctions (i.e., one-dimensional $Cd_{0.5}Zn_{0.5}S$ nanorod

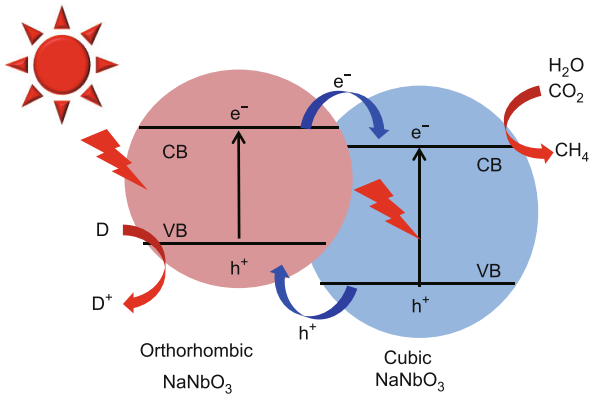

Figure 8 Proposed electron transfer in $NaNbO_3$-based junctions and the surface photocatalytic reactions.

homojunctions [213], a tungsten-doped $BiVO_4$ homojunctions [214], alpha-/gamma-Bi_2O_3 [215] homojunctions, and p–n Cu_2O [216] homojunctions) have been reported recently, and all of them exhibited much higher photocatalytic activity or photovoltaic efficiency than the pure phase. However, there have been no reports about the application of visible-light-driven homojunctions in the CO_2 photocatalytic reduction. Therefore, it is of great interest and worth noticing at this point that the heterophase junctions based on visible-light-driven semiconductors might have potential applications in the CO_2 photoreduction under visible light irradiation.

Up to now, there are also many hetero-structured semiconductor systems applied in the fields of photochemical reduction of CO_2. Among them, TiO_2-based semiconductor composites have been extensively studied. The ordered mesoporous CeO_2-TiO_2 composites exhibited excellent photocatalytic activity in the reduction of CO_2 with H_2O to CH_4 and CO under simulated solar irradiation, which were about ten and three times higher than that of commercial P25, respectively, due to the enhanced separation of photogenerated electrons and holes [217]. TiO_2/ZnO composites showed much higher performance in the photoreduction of CO_2 into CH_4, which was about six times higher than that of commercial P25. The enhancement in CO_2 reduction performance of the hybrid TiO_2/ZnO composites was probably resulted from a faster diffusion transport of photogenerated electrons, decrease of electron-hole recombination rate and increase of specific surface areas [41]. 1.0 wt% CuO-loaded TiO_2 showed the highest photocatalytic reduction activity of CO_2 to methyl formate in methanol solution, which was about two times higher than that of TiO_2 [95]. The methane production rate over hetero-structured CuO-$TiO_{2-x}N_x$ hollow nanocubes was 2.5 times faster than that of Degussa P25 TiO_2 when measured under the same conditions [218]. In addition, the CH_4 production yield of optimal In_2O_3-g-C_3N_4 hybrids with 10 wt% In_2O_3 (76.7 ppm) is three to four times higher than that of pure g-C_3N_4 or In_2O_3, due to effective charge separation and longer lifetime of the photogenerated charge carriers [219]. The hetero-structured Bi_2S_3/CdS [60] and Cu_2O/SiC [52] photocatalysts have been used to photoreduction of CO_2 to CH_3OH under visible-light irradiation. In contrast to the single semiconductor, the hetero-structured photocatalysts showed a 2- or 3-fold enhancement in the photoactivity for CO_2 reduction. It can be mainly ascribed to the improved charge separation. However, challenges still remain in the further promotion of electron transfer between two semiconductors. In future studies, it is of great interest to construct the core/shell structured [220–222] and two-dimensional layered heterojunction systems [223] because of the larger contact area and better surface passivation effects.

Semiconductor/nano-carbon heterojunctions

Another strategy for improving charge separation is coupling semiconductor with nano-carbon materials, which can greatly enhance the collection and transfer of photogenerated electrons and reduce the charge recombination due to the excellent properties of nano-carbon materials. Among carbon-based supports, carbon nanotubes (CNT) and graphene are excellent candidates due to their outstanding properties. CNT possesses many unique properties such as a large electron-storage capacity, good electron conductivity, good chemical stability, excellent mechanical strength, a large specific surface area (> 150 $m^2\ g^{-1}$), and mesoporous character which favors the diffusion of reacting species [224–226]. Consequently, as a good support for semiconductors, CNT has been widely used to construct semiconductor–CNT nanocomposite photocatalysts in the past few years [227,228]. However, there are very restricted reports on semiconductor-CNT nanocomposite photocatalysts for photocatalytic CO_2 reduction. The multi-walled CNTs (MWCNTs) supported TiO_2 composite catalysts prepared by the sol-gel method lead to the main formation of C_2H_5OH, while HCOOH is found to be the major product on the sample prepared by the hydrothermal method [229]. Chai and his coworkers [230,231] reported that the CNT@Ni/TiO_2 and MWCNT/TiO_2 core-shell nanocomposites showed excellent photocatalytic activity towards CH_4 synthesis as compared to TiO_2 and Ni/TiO_2 under visible light illumination, on which the maximum yields of CH_4 were 0.145 and 0.17 μmol $g_{cat}^{-1}\ h^{-1}$, respectively.

Graphene, a single layer of graphite, possesses a unique two-dimensional structure, high conductivity (~5,000 $W\ m^{-1}\ K^{-1}$), superior electron mobility (200,000 $cm^2\ V^{-1}\ s^{-1}$), and extremely high specific surface area (~2,600 $m^2\ g^{-1}$), and can be produced on a large scale at low cost [232–234]. Since the pioneering studies by Kamat and coworkers [235,236], semiconductor/graphene-based nanocomposites have attracted a lot of attention in different fields due to their good electron conductivity, large specific surface area and high adsorption [222,237–240].

There were a large number of reports about the semiconductor-graphene nanocomposite photocatalysts for CO_2 photoreduction. Interestingly, the graphene oxide can be directly applied as a promising photocatalyst for CO_2 to methanol conversion. The largest conversion rate of photocatalytic CO_2 to methanol on modified graphene oxide is 0.172 μmol $g_{cat}^{-1}\ h^{-1}$ under visible light, which is 6-fold higher than that of pure TiO_2 [241]. The nanocomposites based on the less defective solvent-exfoliated graphene exhibit a significantly larger enhancement in CO_2 photoreduction, especially under visible light [242]. The rates of CO and CH_4 formations over the $Ti_{0.91}O_2$-graphene hollow spheres were 8.91 and 1.14 μmol $g^{-1}\ h^{-1}$, respectively,

which was about 5 times higher than that over the $Ti_{0.91}O_2$ [243]. Meanwhile, the TiO_2-graphene 2D sandwich-like hybrid nanosheets were also synthesized by a one-step hydrothermal method in a binary ethylenediamine (En)/H_2O solvent. The results showed that the synergistic effect of the surface-Ti^{3+} abundant TiO_2 and graphene favors the generation of C_2H_6, and the yield of the C_2H_6 increases with increasing the content of incorporated graphene [244]. In addition, the hierarchically mesostructured TiO_2/graphitic carbon composite photocatalyst exhibited considerably higher activity in the photocatalytic reduction of CO_2 with H_2O than a mesostructured anatase TiO_2 prepared by a sol-gel method [245]. The NiO_x-Ta_2O_5-rGO (reduced graphene oxide) containing 1 wt% graphene (G1.0) displayed the highest activity for photoreduction of CO_2 to CH_3OH, which was 3.4 times higher than that of corresponding photocatalyst without graphene (G0) under the same conditions, due to promoted electron transfer and collecting characteristics of rGO [246]. The photocatalytic activity of graphene-WO_3 (GW) nanobelt composites is higher than that of graphene oxide (GO), WO_3 and P25 TiO_2 because of the elevated conduction band of WO_3 [247]. In another example, Cu_2O/rGO composites exhibit a high activity for CO_2 photoreduction to CO, which is about 6 and 50 times higher than that of the optimized Cu_2O and Cu_2O/RuO_x junction, respectively. The enhanced activity is attributed to the efficient charge separation and transfer and the protection function of rGO [248]. Similarly, the CH_4-production rate of a rGO-CdS nanorod composite photocatalyst was increased 10-fold compared with that of the pure CdS nanorods, which was even better than that of an optimized Pt-CdS nanorod photocatalyst under the same reaction conditions [108]. The rGO sheets in the composites not only promote the surface trapping and efficient separation of photo-generated charge carriers as an electron acceptor and transporter (as presented in Fig. 9), but also

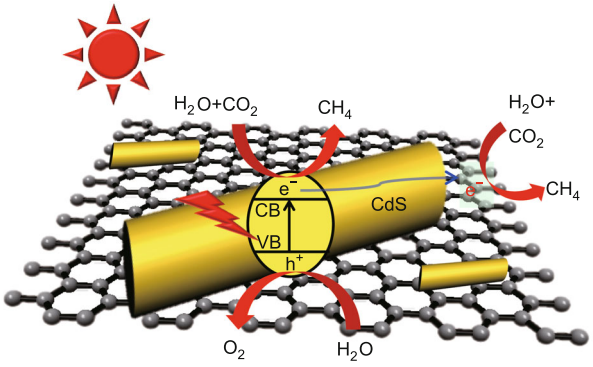

Figure 9 Schematic illustration of the charge transfer and separation in the RGO-CdS nanorod system under visible-light irradiation.

enhance the adsorption and activation of CO_2 molecules, thus boosting the photocatalytic efficiency of the composite photocatalysts.

In addition, it is worth noticing that the defects of graphene in carbon/TiO_2 nanocomposite photocatalysts also play a significant role in the photocatalytic reduction of CO_2. Liang *et al.* [242] demonstrated that the less defective solvent-exfoliated graphene (SEG) resulted in a larger enhancement in the activity for photoreduction of CO_2 to CH_4, compared to the solvent-reduced graphene oxide (SRGO). It was found that the optimized graphene/TiO_2 nanocomposites exhibit approximately 7-fold improvements in the photoreduction of CO_2 compared with TiO_2 alone under visible illumination [242].

Enhanced adsorption and activation of CO_2

Effective adsorption and activation of CO_2 is a key step for improving the efficiency for CO_2 reduction. The adsorption and photoinduced activation of CO_2 on stoichiometric and oxygen-deficient TiO_2 surfaces have been theoretically [39,81,249,250] and experimentally studied [251,252]. Recently, some interesting results have been reported through the quantum chemical calculations. Several CO_2 adsorption sites on the predominant anatase TiO_2 (101) surface and on nanoclusters can be identified using first-principles calculations [39,249,253]. Thus, to well understand the key factors affecting adsorption and photoinduced activation of CO_2, a combination of experimental and computational studies is also highly expected.

Increased surface area for CO_2 adsorption

For TiO_2, it is clear that the adsorption isotherms of CO_2 on pure and nitrogen modified TiO_2 photocatalysts can be well described by the Freundlich adsorption equation [63,254], which indicates that adsorption of CO_2 onto TiO_2 photocatalysts is a favorable physical process. Therefore, the enhancement in adsorption capacity of TiO_2 photocatalyst for CO_2 can be realized through increasing its surface area.

In recent years, it was widely reported that most metal-organic frameworks (MOFs) with super-high surface areas exhibit excellent adsorption capacity for CO_2 [255,256]. Interestingly, MOFs are also a class of potential semiconductors [257], which could be also directly applied in the photocatalytic CO_2 reduction as photocatalysts [258–261]. For example, Fu *et al.* [259] reported that a photoactive Ti-containing metal-organic framework, NH_2-MIL-125(Ti), exhibited a good photocatalytic activity for reduction of CO_2 to formate anion under visible light irradiation. The Re complexes derivatized UiO-67 served as an active catalyst for photocatalytic CO_2 reduction to CO with a total turnover number (TON) of 10.9, which was three times higher than that of the homogeneous Re complexes [260].

Wang *et al.* [262,263] demonstrated that a cobalt-containing zeolitic imidazolate framework (Co-ZIF-9) as a robust MOF co-catalyst could achieve the photocatalytic conversion of CO_2 to CO by using a Ru-based dye or CdS as the light harvester. It was suggested that the Co-ZIF-9 could not only promote the CO_2 capture and reduction catalysis, but also play a crucial role in improving electron transfers in the light harvester system [262,263]. Thus, it is naturally expected that MOFs as good supports can greatly promote the activity of a photocatalyst for CO_2 photoreduction to fuels due to their excellent adsorption capacity and photocatalytic reduction the activity for CO_2. Recently, it was first verified that the addition of 25 wt% ZIF-8 to Zn_2GeO_4 nanorods could achieve a 3.8-fold enhancement in adsorption capacity for CO_2 dissolved in water and a 62% enhancement in photocatalytic activity for the reduction of CO_2 to CH_3OH [264]. Therefore, as molecularly tunable and recyclable photocatalysts in CO_2 reduction, MOFs deserve more attention. However, the instability of MOFs in some conditions should be improved for their practical applications.

Increased basic sites for CO_2 adsorption

Apart from increasing the surface area for CO_2 adsorption, another widely selected strategy to maximize adsorption of acidic CO_2 molecules is to introduce functional basic groups (or basic sites) on the material surface of porous materials [255,256,265]. For example, the amine-functionalization of TiO_2 NPs exhibited significantly enhanced activities for photoreduction of CO_2 into methane and CO due to improved chemisorption and activation of CO_2 and charge transfer from excited TiO_2 [266]. At this regard, it is expected that mesoporous C_3N_4 photocatalyst should have excellent adsorption selectivity and capacity for CO_2 because of rich nitrogen-containing groups on the surface of C_3N_4 [70]. However, so far, there are few reports about the CO_2 adsorption and photoreduction on C_3N_4 [69,109,110,267]. Thus, more efforts should focus on the adsorption and photocatalytic reduction CO_2 on mesoporous g-C_3N_4 photocatalysts in future studies. Furthermore, the nitrogen-doped carbon nanotubes (CNTs) or graphene have been extensively used as an efficient electrocatalyst for hydrogen or oxygen evolution [268–270], because nitrogen impurities can function as catalytic sites. Interestingly, the nitrogen-containing sites are also potential active sites for CO_2 adsorption. Thus, it is highly expected the promising nitrogen-doped CNTs or graphene can be deeply studied and applied in photocatalytic reduction of CO_2 due to the synergistic effect of their good electron conductivity and potential adsorption ability for CO_2.

In addition, the loading of basic sites on the surface of photocatalysts can also be achieved using the solid basic (hydro)oxides such as NaOH, MgO and ZrO_2. Ye and coworkers [271] demonstrated that the surface modification of TiO_2 with NaOH could greatly enhance the CO_2 adsorption, activation, thus leading to highly effective photoreduction of CO_2 into CH_4 without loading any noble metal co-catalysts. Kohno *et al.* [272,273] reported that the photocatalytic reduction of CO_2 to CO can be achieved over MgO. However, the mechanism of the photoreduction of CO_2 on MgO cannot be explained by the conventional band theory because MgO is not a semiconductor [272]. Thus, a new concept for photocatalytic reduction of CO_2 over an insulating material was proposed. It is believed that a CO_2^- radical can form by activating CO_2 adsorbed on MgO under photoirradiation. Then it was reduced to the surface bidentate formate by H_2 or CH_4 in the dark. The surface bidentate formate as photoactive species can further reduce CO_2 in the gas phase to CO under photoirradiation. The mechanism can also be used to explain the photocatalytic reduction of CO_2 over ZrO_2 [274]. Recently, the addition of MgO modifier onto TiO_2 [275–277] was found to be capable of significantly enhancing the activity for photocatalytic reduction of CO_2. The proposed mechanisms of the MgO layers and Pt NPs over TiO_2 for photocatalytic reduction of CO_2 in the presence of H_2O were shown in Fig. 10. Clearly, the MgO layers on TiO_2 surfaces not only enhance the adsorption of CO_2 as basic sites, but also can capture the holes and promote charge separation. More importantly, it also can inhibit the reoxidation of products owing to avoiding direct contact of products and TiO_2 [276]. In addition to MgO, ZrO_2 [278], Ga_2O_3 [279] and layered double hydroxides [280–282] also have great potentials to function as modifiers to enhance the activities for photocatalytic reduction of CO_2 over semiconductor photocatalysts.

Important factors affecting CO_2 activation

The surface oxygen vacancies play very important roles in governing the adsorption, activation and dissociation of

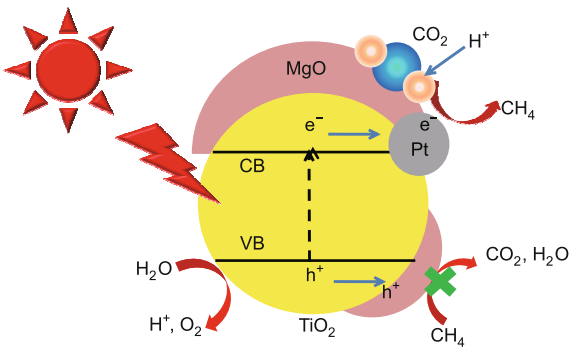

Figure 10 Proposed mechanisms of the MgO layers and Pt NPs over TiO_2 for photocatalytic reduction of CO_2 in the presence of H_2O.

CO_2, which provide not only an electronic charge (Ti^{3+}) but also the sites for the adsorption of oxygen atoms from CO_2 [283]. It was even demonstrated that CO_2^- species, generated upon an electron attachment to CO_2, are spontaneously dissociated into CO on defective Cu(I)/TiO_{2-x} at room temperature even in the dark [283]. Indrakanti *et al.* [249] performed the excited-state *ab initio* calculations of CO_2 adsorbed on clusters from the (010), (101), and (001) anatase surface planes. The calculated results indicated that oxygen vacancies may act as the active sites for CO_2 photoreduction, whereas the activation of CO_2 can't be achieved on the stoichiometric TiO_2 surfaces. Meanwhile, the adsorption of CO_2 and temperature programmed desorption (TPD) experiments also demonstrated that chemical adsorption of CO_2 can be improved through increasing the oxygen vacancy in $SrTiO_3$, which would lower the activation barrier of CO_2 and favor the photoreduction of CO_2 to hydrocarbon fuels [284]. It is expected that the oxygen vacancies, and the adsorption and activation of CO_2 on the defective surface of a given photocatalyst can be experimentally investigated in detail, which may provide necessary information for designing highly efficient photocatalysts.

It is also clear that the polarity and dielectric constant of solvents, acid–base properties of supports and the hydrophobic-hydrophilic nature of catalysts have significant influences on the activation of CO_2, the stability of CO_2^- radical anion and the catalytic activity and selectivity [59,84,181,285]. For example, through loading TiO_2/Pd, CuO/ZnO and Li_2O-TiO_2 on the supports of magnesium oxide, aluminium oxide and silicon dioxide, it was found that the conversion of CO_2 to C_1–C_3 compounds took place preferentially on basic oxide supported systems, and acidic oxide supported catalysts showed more selectivity to C_1 compounds [84]. Consequently, the acidic oxide such as SiO_2 was generally used to obtain the C_1 compounds in most studies. The formation of CH_4 and CH_3OH from CO_2 photoreduction with gaseous and liquid water was observed over Ru-TiO_2/SiO_2 [83] and TiO_2-containing porous SiO_2 thin film [286], respectively. It is also evident that the selective formation of CH_3OH from CO_2 photoreduction with gaseous water increases rapidly with decreasing the surface concentration of hydroxyl groups [286]. Very recently, it was reported that the selectivity for photoreduction of CO_2 can be tailored by controlling the band structure of a g-C_3N_4 photocatalyst [287]. Thus, it is clear that the band structure, surface state and sites (e.g., the chemistry of CO_2 adsorption, oxygen vacancies, isolated Ti-species, acid–base properties and the hydrophobic-hydrophilic nature) played very crucial roles in the photoinduced activation of CO_2 [39,88,288–290].

Meanwhile, the water vapor adsorption can be also tuned through managing the surface area and pore structure of porous materials [291–293]. It is worth noticing that the SiO_2-pillared HNb_3O_8 photocatalysts also exhibit a 6-fold enhancement in the photocatalytic activity for CO_2 reduction due to increased adsorption ability for water vapor molecules on SiO_2 [294]. However, an excess amount of H_2O will suppress the reaction. The optimum mole ratio of H_2O/CO_2 for CO_2 photoreduction over highly dispersed TiO_2 anchored on porous Vycor glass was found to be about 5 [295]. Recently, efficient high-rate sunlight-driven conversion of diluted CO_2 into light hydrocarbons in gas phase was also achieved by coupling coaxial Cu-Pt bimetallic coatings with these TiO_2 nanotube arrays as catalysts at room temperature [188]. Therefore, for the photocatalytic reduction of CO_2 by water vapor, control of CO_2 and H_2O adsorption capacity of photocatalysts and the ratio of H_2O to CO_2 is of great importance to optimize the photocatalytic activity and selectivity in future studies.

Accelerated CO_2 reduction kinetics

Developing mesoporous photocatalysts

Developing mesoporous semiconductor photocatalysts has become a popular strategy to effectively increase the active sites, surface area and light harvesting. The mesoporous structure can also facilitate access of reactants to the surface active sites and improve multiple scattering. All these factors can subsequently maximize the activity for photoreduction of CO_2. Typically, the micro/mesoporous Zn_2GeO_4 with crystalline pore-walls [296] and mesoporous zinc germanium oxynitride [176] exhibited much higher activities for CO_2 photoreduction (about 2.5–5.0 times) than the corresponding samples obtained by a solid state reaction, respectively, due to the increased surface area and improved pore structure. The mesoporous $ZnGa_2O_4$ prepared by a reactive templating route at room temperature also exhibited a higher activity (CH_4: 5.3 ppm h^{-1}) than $ZnGa_2O_4$ (CH_4: trace) obtained by a solid state reaction [297]. The indium hydroxide ($In(OH)_3$) sample with mesoporous structure is about 20 times higher in efficiency for the photoreduction of CO_2 to CH_4 than that of sample without mesoporous structure [298]. With respect to the bulk NPs, the porous gallium oxide exhibits the enhanced photocatalytic activity of conversion of CO_2 into CH_4, which is mainly due to the 300% higher CO_2 adsorption capacity, as well as the 200% increased surface area [299]. For mesoporous graphitic C_3N_4, it was revealed that the photoactivity for CO_2 reduction to formic acid was strongly dependent on its specific surface area and crystallinity rather than the pore size and the volume [300]. Similarly, the enhancements of photocatalytic performance for CO_2 reduction over mesoporous composites (CeO_2-TiO_2 [217] and TiO_2/ZnO [41]) were also observed in a different group. However, the direct syn-

thesis of highly crystalline mesoporous transition-metal oxides that are thermally stable and well-ordered remains a major challenge [301]. Another challenge is to prepare multimetallic oxide mesoporous materials and their oxynitride. Particular emphasis should be placed on preparing these kinds of active materials by soft chemical methods for the application of photoreduction of CO_2 under visible-light irradiation.

Meanwhile, as another effective strategy to develop mesoporous photocatalysts, constructing isolated centers in zeolite matrices (or loading photocatalyst NPs onto zeolites or mesoporous molecular sieves) has also been widely investigated. Zeolites exhibit unique nanoscaled porous structures and ion exchange properties. Zeolites are often employed as organizational media or supports for entrapped or adsorbed transition-metal catalysts and photocatalysts [302]. Therefore, zeolites have been widely utilized in the design of efficient photocatalytic systems for CO_2 photoreduction. So far, the highly dispersed Ti-oxides in silica matrices are one of the best performing photocatalysts in direct CO_2 reduction to hydrocarbons, pioneered by Anpo and his co-workers in the 1990s [303]. The titanium oxide anchored on Y-zeolite exhibits the highest photocatalytic activity and the highest selectivity for the formation of CH_4 and CH_3OH, whereas CO is formed as a main product on the titanium oxide anchored on ZSM-5 [295]. It is clear that the activity and selectivity of photocatalysts for different products strongly depend on the chemical nature of the supports. Yet, the microporous structure of zeolites is not beneficial for the improvement of photocatalytic activity. Thus, a variety of mesoporous molecular sieves (MCM-41, MCM-48, KIT-6, FSM-16 and SBA-15) are also applied in photocatalytic CO_2 reduction [285,290,295,304–309]. Ti-MCM-41 and Ti-MCM-48 mesoporous zeolite catalysts exhibited high photocatalytic reactivity for the reduction of CO_2 with H_2O at 328 K to produce CH_4 and CH_3OH in the gas phase. Especially Ti-MCM-48 with a large pore size and three-dimensional channels exhibited the highest reactivity for CH_4 production, which was almost ten times higher than that of bulk TiO_2 [304]. The further results showed that the dispersed TiO_2 within mesoporous FSM-16 and SBA-15 exhibited much higher photocatalytic activities for CO_2 reduction than other supports. Furthermore, Ti-containing Ti-KIT-6, Ti-FSM-16 and Ti-SBA-15 prepared by hydrothermal synthesis also showed very high yields in methane or/and methanol, respectively. In particular, the photocatalytic reaction yields of the Ti-SBA-15 catalyst for CH_4 formation under UV light are over 240 times higher than those of the TiO_2 catalyst and the yields for CH_3OH formation increase remarkably over 4000 times [290,310]. More recently, a new photocatalyst, Ti-TUD-1, showed a 30% increase in the total hydrocarbons produced by CO_2 photoreduction, as compared with Ti-SBA-15 [311]. In a word, highly dispersed titanium oxide in mesoporous silica materials (KIT-6, FSM-16, SBA-15 and TUD-1) leads to relatively high yield in CH_4 or/and CH_3OH, which is a promising candidate for CO_2 photoreduction.

Recently, much attention has been directed at monolayered zeolites [312] and zeolite nanosheets [313–315] which can increase the external to internal surface ratio and thus can enhance the catalytic activity. However, this kind of layered zeolite nanosheets has not been used in photocatalysts. Maybe zeolite nanosheets can provide a new strategy for designing highly efficient photocatalysts for photocatalytic reduction of CO_2.

Loading CO_2 reduction co-catalysts

It is generally believed that the co-catalysts can extract the photogenerated charge carriers from semiconductors, provide reaction sites, lower the electrochemical overpotentials associated with the multielectron water oxidation and CO_2 reduction reactions, and decrease the activation energy for gas evolution [316,317]. Another function is to provide a junction/interface between the co-catalyst and the semiconductor to enhance electron–hole separation or charge transport [317,318].

For photoreduction of CO_2, the loaded co-catalysts could serve as electron traps to enhance the separation of the photogenerated electron-hole pairs and hence improve the photocatalytic activity and selectivity for CO_2 reduction. Generally, Pd, Pt and Au can selectively reduce CO_2 into CH_4 products. Ishitani *et al.* [136] first systematically studied the photoreduction of CO_2 on a series of metal-deposited TiO_2 and found that depositing metals (Pd, Rh, Pt, Au, Cu_2O, etc.) on TiO_2 photocatalysts can greatly boost their photocatalytic activities for CO_2 reduction to CH_4 (in decreasing order). The addition of Pt onto the highly dispersed titanium oxide catalysts promotes the charge separation which leads to an increase in the formation of CH_4 in place of CH_3OH [305]. Pt NP/TiO_2 nanotube composite greatly promoted the photocatalytic conversion of CO_2 and water vapor into methane due to a large number of active reduction sites from the homogeneous distribution of metal co-catalyst NPs over the TiO_2 nanotube array surface [186]. A unique one-dimensional (1D) structure of TiO_2 single crystals coated with ultrafine Pt NPs (NPs, 0.5–2.0 nm) exhibited extremely high CO_2 photoreduction efficiency with selective formation of methane (the maximum CH_4 yield of 1361 μmol g_{cat}^{-1} h^{-1}) [319]. A similar result was also observed on the Pt-C_3N_4 system [201]. The highest yield of CH_4 was obtained on the g-C_3N_4 loaded by about 1 wt% Pt. Here, Pt NPs not only improve the transfer of photogenerated electrons and the activity for photocatalytic reduction of CO_2 as a co-catalyst, but also promote

the oxidation of reduction products (as shown in Fig. 11) [201]. The loading of Pd (> 0.5 wt %) on TiO_2 can suppress the CO formation and promote the CH_4 formation [320].

In addition, it is worth noticing that the bimetallic co-catalysts systems (Cu and Pt) exhibited better activities for CO_2 reduction than single metallic co-catalysts systems. For example, a hydrocarbon production rate of 111 ppm cm^{-2} h^{-1}, or ≈ 160 μL g^{-1} h^{-1}), is obtained when the nitrogen-doped TiO_2 nanotube array samples are loaded with both Cu and Pt NPs. It was pointed out that this rate was at least 20 times higher than that in the previously published reports [97]. The mechanisms for photocatalytic CO_2 conversion to fuels over this composite photocatalyst were illustrated in Fig. 12. In another example, a bimetallic co-catalyst of $Cu_{0.33}$-$Pt_{0.67}$ was loaded on the double-walled TiO_2 nanotube for the photoreduction of diluted CO_2 to CH_4 (1% in N_2), an average hydrocarbon production rate of 6.1 mmol m^{-2} h^{-1} was realized under AM 1.5 one-sun

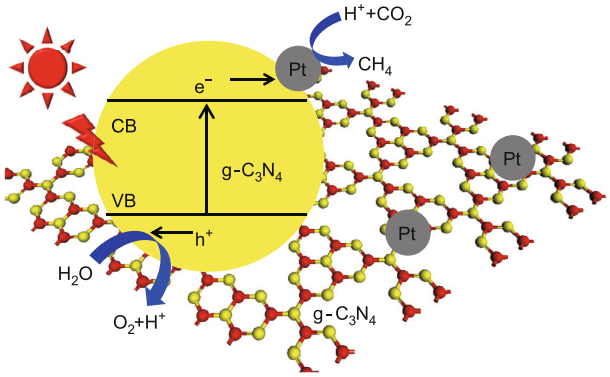

Figure 11 Schematic illustration of CO_2 photoreduction in the Pt/g-C_3N_4 system under visible light irradiation.

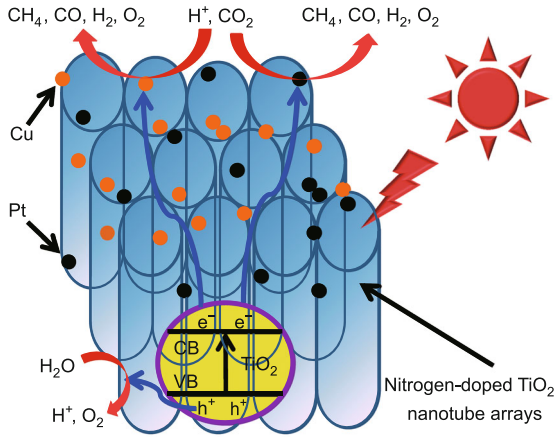

Figure 12 Mechanisms for photocatalytic CO_2 conversion to fuels using nitrogen-doped TiO_2 nanotube arrays loaded with Cu and Pt co-catalyst NPs.

illumination [321]. However, the enhancement mechanism of bimetallic co-catalysts is still unclear. Thus, a deeper understanding and investigation of these bimetallic co-catalysts might be needed for their further application in this field.

Meanwhile, Au and Ag-loaded TiO_2 photocatalysts have also been widely studied. For a leaf-architectured artificial photosynthetic system of $SrTiO_3$, Au exhibits the best performance as a suitable co-catalyst for both CO and CH_4 selectivity [11]. The nanoscale TiO_2 particles embedded in the hydrophilic cavities of Nafion membrane films significantly improved photoconversion of CO_2 to methanol when coated with silver [322]. Ag co-catalyst-loaded $ALa_4Ti_4O_{15}$ (A = Ca, Sr, and Ba) photocatalysts showed better activities for CO_2 reduction to CO and HCOOH without any sacrificial reagents [323].

Furthermore, RuO_2 has also proved to be a good co-catalyst for CO_2 photoreduction. The maximum CH_3OH yield observed was about 118.5 μmol g^{-1} h^{-1} in the presence of $RuO_2/Cu_xAg_yIn_zZn_kS_m$ photocatalysts under H_2 atmosphere [175]. The generation rate of CH_4 over meso-$ZnGa_2O_4$ could be significantly enhanced by loading 1 wt% RuO_2 as co-catalyst to improve separation of the photogenerated electron–hole pairs [297]. The rate of CH_4 generation over the Zn_2GeO_4 nanoribbons could also be significantly enhanced by loading of Pt or RuO_2 and especially by co-loading of Pt and RuO_2 as co-catalysts [195].

Besides noble metal co-catalysts mentioned above, it is indispensable to search for cheap, earth-abundant and highly efficient co-catalysts for photocatalytic reduction of CO_2 [324]. Generally, the first-row transition metals such as Co, Ni, Mn, Fe and Cu, have been recognized as good candidates for practical applications [325,326]. For example, copper as an earth-abundant co-catalyst has been extensively used in the photoreduction of CO_2. In most cases, the active species on Cu-loaded TiO_2 is Cu_2O, which not only greatly enhances the photochemical production of CH_3OH, CO and CH_4 from the CO_2 and gaseous H_2O system [54,86,327], but also greatly improves the photocatalytic activity for CO_2 reduction to methanol in liquid phase. The copper cluster is an effective electron trapper, and able to reduce the recombination of electron–hole pairs [55,133]. However, higher Cu loading gave a lower rate of methanol yield because of the masking effect of Cu_2O clusters on the TiO_2 surface [132,133]. Consequently, it is generally believed that CO_2 can be selectively reduced to methanol in an aqueous solution under light irradiation due to the Cu_2O or CuO species on the TiO_2 surface [54,55,131,133,218,308,328].

In addition, NiO NPs were also usually loaded on different semiconductors as a co-catalyst to enhance their photocatalytic activity for CO_2 reduction. The NiO_x co-cat-

alysts loaded on the surface of $InTaO_4$ can slightly increase the methanol yield from CO_2 reduction [121–123]. Thus, to further enhance the activity for CO_2 reduction, core/shell Ni/NiO co-catalysts were also constructed and used in the photocatalytic conversion of CO_2 [122,246,329]. In particular, the methanol yield over the Ni@NiO core/shell structure-modified nitrogen-doped $InTaO_4$ photocatalyst is about three times higher than that of pure $InTaO_4$. It is believed that the co-catalyst loading not only dramatically enhances absorbance, but also efficiently avoids electron–hole recombination [124].

Unfortunately, the molecular O_2 and H_2 had not been quantitatively measured in these reports. It is very important to detect the molecular O_2 and H_2 for the Ni-base co-catalysts systems because NiO_x is also an efficient co-catalyst for photocatalytic hydrogen generation from water splitting. Therefore, it is suggested that the molecular O_2 and H_2 should also be detected when the NiO and core/shell Ni/NiO co-catalysts were used for the photocatalytic reduction of CO_2.

However, nowadays, there were seldom reports on the photocatalytic reduction of CO_2 by loading two different co-catalysts for water oxidation and CO_2 reduction. Therefore, special attention should be given in future studies to the systems with two separated co-catalysts for water oxidation and CO_2 reduction [330].

Improving water oxidation kinetics

Generally, to increase the photocatalytic activities of semiconductors and prevent the oxidation of the reduction products in liquid phase, some highly efficient electron-donor sacrificial agents including EDTA, Na_2SO_3, acetonitrile, dichloromethane, iso-propyl alcohol, alcohols and amines were also widely used in many photocatalytic reduction systems. It can be expected that these electron donors will not compete with CO_2 in the trapping of the electrons in the CB since they are more difficult to be reduced as compared to water. For instance, Richardson *et al.* [12] also demonstrated a very interesting concept using a tertiary amine as an recycling electron donor to combine CO_2 photoreducton with water splitting for improving the overall efficiency.

However, water is not a real electron donor in the presence of sacrificial reagents. In theory, the oxygen-evolution half-reaction is an important part of the process of CO_2 photoreduction [331–335], as improvements of water oxidation must be favorable for the efficient separation of the photo-generated carriers and the enhancement in the photocatalytic activity for the reduction of CO_2. Especially, the water oxidation reaction is an important bottleneck for both photocatalytic H_2 production and CO_2 reduction because this reaction is considerably more difficult and complicated. It requires a four-electron oxidation of two water molecules coupled to the removal of four protons to form a relatively weak oxygen-oxygen bond [336,337]. Although it is well accepted that the CO_2 photoreduction process (the reduction half-reaction) is accomplished by O_2 and H_2O_2 formation, which comes from the oxidation of water (the oxidation half-reaction) [5,89,92,338], or water splitting [90,143,252,339], many researchers only measured the products from the reduction of CO_2 and always ingored the measurement of the products (O_2 and H_2) from water splitting reaction. The evolution rate of O_2 from the photoreduction of CO_2 with H_2O was first studied by Ogura *et al.* [340]. In particular, water oxidation products (O_2) were also detected during the photoreduction of CO_2 over ZrO_2 [341], $KCaSrTa_5O_{15}$ [342], $KTaO_3$ [343] and $ALa_4Ti_4O_{15}$ (A = Ca, Sr, and Ba [323]) photocatalysts in water. Importantly, evolution of (H_2 + CO) and O_2 in a stoichiometric amount (2:1 in a molar ratio) was observed in the absence of sacrificial reagents, further indicating that water could function as a reducing reagent (an electron donor) for the CO_2 reduction [323]. Consequently, it is of great significance to examine the amounts of oxygen from the CO_2 photoreduction with H_2O in future studies. In particular, to identify who is the real electron donor, it is quite necessary that the molecular O_2 should be also quantitatively measured during the photocatalytic reduction of CO_2 [59,117,181,344]. To some extent, O_2 should be especially carefully checked whether they do not form really or may be not detected, remaining adsorbed on the photocatalyst.

Meanwhile, when the photocatalytic reduction of CO_2 is performed in the gas phase with controlled proportion of water vapor as a reductant agent, the photocatalytic activity of semiconductor for CO_2 reduction is much higher than that observed in liquid phase. Therefore, for these reasons, the photocatalytic reduction of CO_2 in the gas phase without using any sacrificial reagent seems to be more promising than that in liquid phase.

So far, there are seldom reports on the application of cobalt-based co-catalysts in the photocatalytic reduction of CO_2. Recently, Lin *et al.* [109] verified that the introduced cobalt oxide (CoO_x) NPs on carbon nitride as reductive and oxidative promoters can improve the photocatalytic activity toward CO_2-to-CO conversion due to the acceleration in the oxidative partner reaction, charge-carrier separation and transfer kinetics. Therefore, loading oxygen-evolution co-catalysts such as Co-Pi, Co_3O_4 and $Fe_{100-y-z}Co_yNi_zO_x$ [345–349] may provide a strategy for improvement of the photocatalytic performance for the reduction of CO_2. Importantly, they not only can enhance the kinetics of water oxidation and suppress the recombination of photo-generated charge carriers, but also can increase the stability of semiconductors.

Suppressed undesirable reaction

Inhibited hydrogen evolution

Selective reduction of CO_2 is another major challenge in the photocatalytic reduction of CO_2 in aqueous solutions because the hydrogen evolution via water reduction is the main competing reaction, which can greatly decrease the efficiency and selectivity for CO_2 reduction. During CO_2 photocatalytic reduction, hydrogen evolution as the side reactions of the photoreduction of CO_2 also usually exists in the systems. The kinetics for CO_2 reduction is unfavorable due to the multi-electron reduction processes, while H_2 evolution generally predominates when thermodynamic conditions for both processes are satisfied [21,22]. Therefore, it is of immense importance to couple CO_2 reduction with water splitting, which is beneficial for finding the rate-determining steps and improving the efficiency and selectivity of CO_2 photoreduction in aqueous solutions. In a certain sense, suppressing the reduction of H_2O to H_2 (a competitive reaction with the reduction of CO_2) can enhance the efficiency and selectivity of CO_2 photoreduction.

Recently, considerable attention has been drawn to this issue. Wang and his coworkers [344] founded that a core-shell structured Pt@Cu_2O co-catalyst on P25 can significantly promote the photoreduction of CO_2 with H_2O to CH_4 and CO and suppress the reduction of H_2O to H_2. The selectivity for CO_2 reduction reached 85%. It was proposed that the Cu_2O shell was capable of providing sites for the preferential activation and conversion of CO_2 molecules in the presence of H_2O and suppressing the reduction of H_2O to H_2, while the Pt core extracts the photo-generated electrons from TiO_2 (Fig. 13).

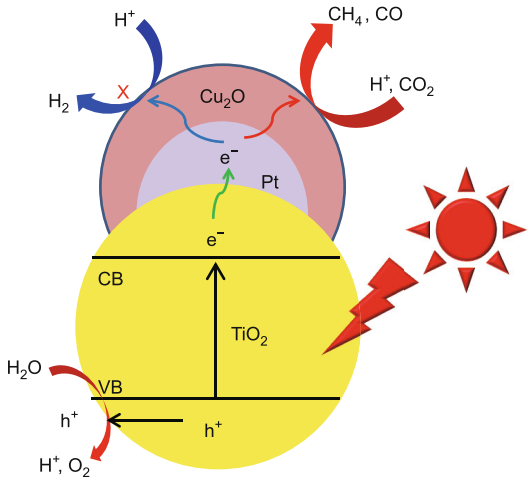

Figure 13 Mechanism of a core-shell structured Pt@Cu_2O co-catalyst on TiO_2 for photocatalytic reduction of CO_2.

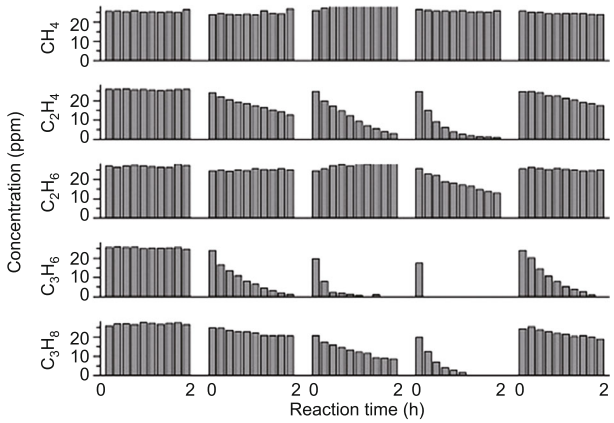

Figure 14 Degradation profiles of the standard hydrocarbons over the prepared samples. The concentrations were recorded every 15 min for the duration of 2 h. Reproduced with permission [311]. Copyright 2014, American Chemical Society.

Inhibited products oxidation

It is a great challenge to separate oxidation and reduction processes on the surface of semiconductor NPs, because many intermediate products of CO_2 reduction cycle adsorbed on the surface could be oxidized, which will reduce overall yield of hydrocarbons and the photocatalytic efficiency [90,350]. The research from the Mul's group [91] demonstrated that the backward reaction, i.e., oxidation of hydrocarbons back to CO_2 and water, proceeds to a significant extent due to the existence of the oxygen from the splitting of water. The further results revealed the importance of evaluating hydrocarbon oxidation in explaining performance of catalysts designed for CO_2 reduction [311]. As displayed in Fig. 14, it is clear that methane only slowly degraded over the catalytic systems within 120 min of illumination whereas the other hydrocarbons (i.e., ethane and propane) were easily degraded, in particular over the Ti-1-Cr-1 sample. Interestingly, the products from CO_2 photoreduction as electron donors are even employed to improve the evolution rate of hydrogen in water splitting, further indicating the reduction product oxidation also exist in the liquid phase [351]. Therefore, it is still a great challenge to minimize hydrocarbon oxidation in process conditions needed for CO_2 reduction.

For CO_2 reduction by water vapor, the control of water vapor pressure appears the challenge, since it is not only the hydrocarbon oxidant but also the reductant for activating CO_2. For CO_2 reduction by liquid water, it is still a challenge to physical separation of oxidation and reduction sites. A thin Nafion layer on Pd-deposited TiO_2 NPs [352] and a proton conducting Nafion membrane [322,353–355] have been used to inhibit the reoxidation of the reduction products and enhance the photosynthetic conversion of

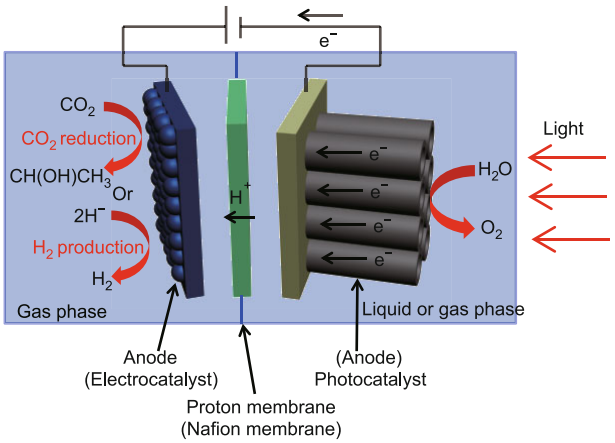

Figure 15 Scheme of the PEC device for CO_2 reduction to fuels and H_2 production. Reproduced with permission [356]. Copyright 2010, RSC Publishing.

CO_2 to corresponding products (mainly methane, ethane, methanol and formic acid) in an aqueous suspension or gas phase. In addition, the PEC conversion of CO_2 to fuel appears to be more promising among various other routes owing to the ability of separating the two half-reactions to avoid reverse processes [17]. For example, to avoid the oxidation of obtained products, the physical separation of the two reactions of water oxidation and CO_2 reduction in a photoanode and cathode, respectively, can be achieved in a newly-designed PEC reactor (as presented in Fig. 15) [356]. Similarly, in another system of PEC reduction of CO_2 into chemicals, Pt-rGO and Pt modified TiO_2 nanotubes (Pt-TNT) performed as cathode and photoanode catalysts, respectively. As a consequence, the separated Pt-rGO exhibited an outstanding activity for CO_2 reduction due to its enhanced adsorption capacity for CO_2 and suppressed oxidation of products [357]. Furthermore, a bifunctionalized TiO_2 film containing a dye-sensitized zone and a catalysis zone as cathode exhibited highly efficient conversion of CO_2 to formic acid, formaldehyde, and methanol through the electron transfer at the CB of TiO_2 under visible light [358]. Importantly, the oxidation of obtained products was prevented via the anode in separated solution. In addition, in Izumi's group, the photocatalytic water oxidation and photocatalytic reduction of CO_2 were successfully integrated in reverse photofuel cells [281,359]. In this new reactor, the oxidation of products from photoreduction of CO_2 can be avoided due to the separate water oxidation and CO_2 reduction, thus leading to an enhanced activity for photoreduction of CO_2 [18]. Therefore, it is interesting to carry out the photocatalytic reduction of CO_2 using a PEC cell.

CONCLUSION AND PROSPECTIVE

In summary, this review highlights the design and fabrication of semiconductor photocatalysts for enhancing photocatalytic efficiency and selectivity of converting CO_2 into useful fuels. Although some significant advances have been achieved in the recent years, the selectivity and yields of the desired products are still rather low and at this point is far from practical application. Therefore, many problems such as the underlying mechanisms of CO_2 photoreduction, the lack of highly efficient photocatalyst and appropriate non-noble metal co-catalyst for special carbonaceous product still need to be clarified in the future.

From our review, it is clear that every step in photocatalysis processes including charge excitation, separation, transport, adsorption and activation of CO_2, CO_2 reduction kinetics and undesirable reactions has significant influences on the overall efficiency of photocatalytic CO_2 reduction. In addition to the photocatalytic properties, adsorption and activation of CO_2, the development of CO_2 reduction electrocatalyst and the suppression of products oxidation are very important to achieve a maximum efficiency. Thus, all the factors should be taken into account and optimized carefully when designing and fabricating multifunctional semiconductor photocatalysts for CO_2 reduction.

Especially, the oxidation of water and products should be also paid more attention in future studies. In photocatalytic systems using semiconductor particles as photocatalysts, it is still a challenge to physical separation of oxidation and reduction sites. A PEC cell seems to be a good choice for the photoreduction of CO_2 in water solution due to the physical separation of water oxidation and CO_2 reduction. The typical strategies in this review can also be used in designing photocathode or photoanode for PEC reduction of CO_2. One possibility for PEC cell is the use of multijunction systems coupling with suitable protective layers or co-catalyst.

The mechanism needs to be deeply investigated in future studies, which still significantly limits the development of the CO_2 photo-reduction. The finding of the rate-determining steps in CO_2 photoreduction is favorable for the design and fabrication of highly efficient and selective photocatalysts. Thus, an in-depth study to understand the surface transformations at the molecular level during CO_2 reduction, including adsorption/desorption of CO_2, surface chemistry and reaction, intermediate products, as well as the role of adsorbed water and carbonates during the reaction is needed in order to reveal the reaction mechanism [90]. To get accurate production yields of the photocatalytic conversion of CO_2, it was essentially important to use isotope labeling of $^{13}CO_2$ as a reactant, which can determine whether the products were derived from CO_2 and not from carbon impurity intermediates [18,320,360]. In addition, the blank tests and different control experiments are highly needed in future studies.

Meanwhile, almost all known non-oxide and many oxide semiconductors suffer from photocorrosion in aqueous electrolytes, which is one of the most fundamental problems that limit the lifetime of all photocatalysts. Therefore, the photostability of the semiconductor should be fundamentally improved to prevent corrosion in the practical application [2,8]. Nanostructured wide-bandgap oxide semiconductor (TiO_2 and titanate mostly) or carbon material coating, surface passivation and co-catalyst loading, have proved to be effective strategies for reducing the photocorrosion of unstable semiconductors.

In a word, all results indicate that the photocatalytic conversion of CO_2 into valuable energy-bearing fuels is still in its infancy, and that breakthroughs for bringing this technology to reality can occur when all these problems and strategies above have been taken into consideration and the photocatalytic system has been well designed.

Received 11 October 2014; accepted 30 October 2014; published online 17 December 2014

1 Lewis NS, Nocera DG. Powering the planet: chemical challenges in solar energy utilization. Proc Natl Acad Sci USA, 2006, 103: 15729–15735
2 Bard AJ, Fox MA. Artificial photosynthesis: solar splitting of water to hydrogen and oxygen. Acc Chem Res, 1995, 28: 141–145
3 Walter MG, Warren EL, McKone JR, *et al.* Solar water splitting cells. Chem Rev, 2010, 110: 6446–6473
4 Chen X, Shen S, Guo L, Mao SS. Semiconductor-based photocatalytic hydrogen generation. Chem Rev, 2010, 110: 6503–6570
5 Inoue T, Fujishima A, Konishi S, Honda K. Photoelectrocatalytic reduction of carbon dioxide in aqueous suspensions of semiconductor powders. Nature, 1979, 277: 637–638
6 Halmann M. Photoelectrochemical reduction of aqueous carbon dioxide on *p*-type gallium phosphide in liquid junction solar cells. Nature, 1978, 275: 115–116
7 Fujishima A. Electrochemical photolysis of water at a semiconductor electrode. Nature, 1972, 238: 37–38
8 Dahl S, Chorkendorff I. Solar-fuel generation: towards practical implementation. Nat Mater, 2012, 11: 100–101
9 Sato S, Arai T, Morikawa T, *et al.* Selective CO_2 conversion to formate conjugated with H_2O oxidation utilizing semiconductor/complex hybrid photocatalysts. J Am Chem Soc, 2011, 133: 15240–15243
10 Sato S, Morikawa T, Saeki S, Kajino T, Motohiro T. Visible-light-induced selective CO_2 reduction utilizing a ruthenium complex electrocatalyst linked to a *p*-type nitrogen-doped Ta_2O_5 semiconductor. Angew Chem Int Ed, 2010, 49: 5101–5105
11 Zhou H, Guo JJ, Li P, *et al.* Leaf-architectured 3D hierarchical artificial photosynthetic system of perovskite titanates towards CO_2 photoreduction into hydrocarbon fuels. Sci Rep, 2013, 3: 1667
12 Richardson RD, Holland EJ, Carpenter BK. A renewable amine for photochemical reduction of CO_2. Nat Chem, 2011, 3: 301–303
13 Kudo A, Miseki Y. Heterogeneous photocatalyst materials for water splitting. Chem Soc Rev, 2009, 38: 253–278
14 Hoffmann M, Martin S, Choi W, Bahnemann D. Environmental applications of semiconductor photocatalysis. Chem Rev, 1995, 95: 69–96
15 Morris AJ, Meyer GJ, Fujita E. Molecular approaches to the photocatalytic reduction of carbon dioxide for solar fuels. Acc Chem Res, 2009, 42: 1983–1994
16 Maeda K, Domen K. New non-oxide photocatalysts designed for overall water splitting under visible light. J Phys Chem C, 2007, 111: 7851–7861
17 Habisreutinger SN, Schmidt-Mende L, Stolarczyk JK. Photocatalytic reduction of CO_2 on TiO_2 and other semiconductors. Angew Chem Int Ed, 2013, 52: 7372–7408
18 Izumi Y. Recent advances in the photocatalytic conversion of carbon dioxide to fuels with water and/or hydrogen using solar energy and beyond. Coordin Chem Rev, 2012, 257: 171–186
19 Dhakshinamoorthy A, Navalon S, Corma A, Garcia H. Photocatalytic CO_2 reduction by TiO_2 and related titanium containing solids. Energy Environ Sci, 2012, 5: 9217–9233
20 Tu W, Zhou Y, Zou Z. Photocatalytic conversion of CO_2 into renewable hydrocarbon fuels: state-of-the-art accomplishment, challenges, and prospects. Adv Mater, 2014, 26: 4607–4626
21 Goren Z, Willner I, Nelson AJ, Frank AJ. Selective photoreduction of carbon dioxide/bicarbonate to formate by aqueous suspensions and colloids of palladium-titania. J Phys Chem, 1990, 94: 3784–3790
22 Willner I, Maidan R, Mandler D, *et al.* Photosensitized reduction of carbon dioxide to methane and hydrogen evolution in the presence of ruthenium and osmium colloids: strategies to design selectivity of products distribution. J Am Chem Soc, 1987, 109: 6080–6086
23 Tong H, Ouyang SX, Bi YP, *et al.* Nano-photocatalytic materials: possibilities and challenges. Adv Mater, 2012, 24: 229–251
24 Park H, Park Y, Kim W, Choi W. Surface modification of TiO_2 photocatalyst for environmental applications. J Photoch Photobio C, 2013, 15: 1–20
25 Bolton JR. Solar fuels. Science, 1978, 202: 705–711
26 Lehn JM, Ziessel R. Photochemical generation of carbon monoxide and hydrogen by reduction of carbon dioxide and water under visible light irradiation. Proc Natl Acad Sci USA, 1982, 79: 701–704
27 Fujita E. Photochemical carbon dioxide reduction with metal complexes. Coordin Chem Rev, 1999, 185: 373–384
28 Bard AJ, Parsons R, Jordan J (eds.). Standard Potentials in Aqueous Solution. New York: CRC press, 1985: 195–197
29 Yahaya AH, Gondal MA, Hameed A. Selective laser enhanced photocatalytic conversion of CO_2 into methanol. Chem Phys Lett, 2004, 400: 206–212
30 Hori Y. Chapter 3, Electrochemical CO_2 reduction on metal electrodes. In: Vayenas CG, White RE, Gamboa-Aldeco ME (eds.). Modern Aspects of Electrochemistry. New York: Springer, 2008: 89–189
31 Schneider J, Jia HF, Muckerman JT, Fujita E. Thermodynamics and kinetics of CO_2, CO, and H^+ binding to the metal centre of CO_2 reduction catalysts. Chem Soc Rev, 2012, 41: 2036–2051
32 Benson EE, Kubiak CP, Sathrum AJ, Smieja JM. Electrocatalytic and homogeneous approaches to conversion of CO_2 to liquid fuels. Chem Soc Rev, 2009, 38: 89–99
33 Song C. Global challenges and strategies for control, conversion and utilization of CO_2 for sustainable development involving energy, catalysis, adsorption and chemical processing. Catal Today, 2006, 115: 2–32
34 Centi G, Perathoner S. Opportunities and prospects in the chemical recycling of carbon dioxide to fuels. Catal Today, 2009, 148: 191–205
35 Kumar B, Llorente M, Froehlich J, *et al.* Photochemical and photoelectrochemical reduction of CO_2. Annu Rev Phys Chem, 2012, 63: 541–569
36 Kanemoto M, Shiragami T, Pac C, Yanagida S. Semiconductor photocatalysis. 13. Effective photoreduction of carbon dioxide catalyzed by zinc sulfide quantum crystallites with low density of surface defects. J Phys Chem, 1992, 96: 3521–3526
37 Nakata K, Fujishima A. TiO_2 photocatalysis: Design and applications. J Photochem Photobiol C, 2012, 13: 169–189

38 Linsebigler A, Lu G, Yates Jr J. Photocatalysis on TiO_2 surfaces: principles, mechanisms, and selected results. Chem Rev, 1995, 95: 735–758
39 Indrakanti VP, Kubicki JD, Schobert HH. Photoinduced activation of CO_2 on Ti-based heterogeneous catalysts: current state, chemical physics-based insights and outlook. Energy Environ Sci, 2009, 2: 745–758
40 Nunez J, O'Shea VAD, Jana P, Coronado JM, Serrano DP. Effect of copper on the performance of ZnO and $ZnO_{1-x}N_x$ oxides as CO_2 photoreduction catalysts. Catal Today, 2013, 209: 21–27
41 Xi GC, Ouyang SX, Ye JH. General synthesis of hybrid TiO_2 mesoporous "French Fries" toward improved photocatalytic conversion of CO_2 into hydrocarbon fuel: a case of TiO_2/ZnO. Chem-Eur J, 2011, 17: 9057–9061
42 Guan GQ, Kida T, Harada T, Isayama M, Yoshida A. Photoreduction of carbon dioxide with water over $K_2Ti_6O_{13}$ photocatalyst combined with Cu/ZnO catalyst under concentrated sunlight. Appl Catal A-Gen, 2003, 249: 11–18
43 Mahmodi G, Sharifnia S, Rahimpour F, Hosseini SN. Photocatalytic conversion of CO_2 and CH_4 using ZnO coated mesh: effect of operational parameters and optimization. Sol Energ Mat Sol C, 2013, 111: 31–40
44 Kuwabata S, Nishida K, Tsuda R, Inoue H, Yoneyama H. Photochemical reduction of carbon dioxide to methanol using ZnS microcrystallite as a photocatalyst in the presence of methanol dehydrogenase. J Electrochem Soc, 1994, 141: 1498–1503
45 Inoue H, Moriwaki H, Maeda K, Yoneyama H. Photoreduction of carbon dioxide using chalcogenide semiconductor microcrystals. J Photoch Photobio A, 1995, 86: 191–196
46 Fujiwara H, Hosokawa H, Murakoshi K, Wada Y, Yanagida S. Surface characteristics of ZnS nanocrystallites relating to their photocatalysis for CO_2 reduction. Langmuir, 1998, 14: 5154–5159
47 Koci K, Reli M, Kozak O, *et al.* Influence of reactor geometry on the yield of CO_2 photocatalytic reduction. Catal Today, 2011, 176: 212–214
48 Aurian-Blajeni B, Halmann M, Manassen J. Photoreduction of carbon dioxide and water into formaldehyde and methanol on semiconductor materials. Sol Energy, 1980, 25: 165–170
49 Sui DD, Yin XH, Dong HZ, *et al.* Photocatalytically reducing CO_2 to methyl formate in methanol over Ag loaded $SrTiO_3$ nanocrystal catalysts. Catal Lett, 2012, 142: 1202–1210
50 Lee WH, Liao CH, Tsai MF, Huang CW, Wu JCS. A novel twin reactor for CO_2 photoreduction to mimic artificial photosynthesis. Appl Catal B-Environ, 2013, 132: 445–451
51 Yamamura S, Kojima H, Iyoda J, Kawai W. Formation of ethyl alcohol in the photocatalytic reduction of carbon dioxide by SiC and ZnSe/metal powders. Electroanal Chem, 1987, 225: 287–290
52 Li H, Lei Y, Huang Y, *et al.* Photocatalytic reduction of carbon dioxide to methanol by Cu_2O/SiC nanocrystallite under visible light irradiation. J Nat Gas Chem, 2011, 20: 145–150
53 Yang TC, Chang FC, Peng CY, Wang HP, Wei YL. Photocatalytic reduction of CO_2 with SiC recovered from silicon sludge wastes. Environ Technol, doi: 10.1080/09593330.2014.960474
54 Li Y, Wang WN, Zhan ZL, *et al.* Photocatalytic reduction of CO_2 with H_2O on mesoporous silica supported Cu/TiO_2 catalysts. Appl Catal B-Environ, 2010, 100: 386–392
55 Tseng IH, Chang WC, Wu JCS. Photoreduction of CO_2 using sol-gel derived titania and titania-supported copper catalysts. Appl Catal B-Environ, 2002, 37: 37–48
56 Bessekhouad Y, Robert D, Weber JV. Photocatalytic activity of Cu_2O/TiO_2, Bi_2O_3/TiO_2 and $ZnMn_2O_4/TiO_2$ heterojunctions. Catal Today, 2005, 101: 315–321
57 Robert D. Photosensitization of TiO_2 by M_xO_y and M_xS_y NPs for heterogeneous photocatalysis applications. Catal Today, 2007, 122: 20–26
58 Fujiwara H, Hosokawa H, Murakoshi K, *et al.* Effect of surface structures on photocatalytic CO_2 reduction using quantized CdS nanocrystallites1. J Phys Chem B, 1997, 101: 8270–8278
59 Liu BJ, Torimoto T, Yoneyama H. Photocatalytic reduction of CO_2 using surface-modified CdS photocatalysts in organic solvents. J Photoch Photobio A, 1998, 113: 93–97
60 Li X, Chen J, Li H, *et al.* Photoreduction of CO_2 to methanol over Bi_2S_3/CdS photocatalyst under visible light irradiation. J Nat Gas Chem, 2011, 20: 413–417
61 Praus P, Kozak O, Koci K, Panacek A, Dvorsky R. CdS NPs deposited on montmorillonite: preparation, characterization and application for photoreduction of carbon dioxide. J Colloid Interf Sci, 2011, 360: 574–579
62 Chaudhary YS, Woolerton TW, Allen CS, *et al.* Visible light-driven CO_2 reduction by enzyme coupled CdS nanocrystals. Chem Commun, 2012, 48: 58–60
63 Li X, Liu HL, Luo DL, *et al.* Adsorption of CO_2 on heterostructure CdS(Bi_2S_3)/TiO_2 nanotube photocatalysts and their photocatalytic activities in the reduction of CO_2 to methanol under visible light irradiation. Chem Eng J, 2012, 180: 151–158
64 Barton EE, Rampulla DM, Bocarsly AB. Selective solar-driven reduction of CO_2 to methanol using a catalyzed *p*-GaP based photoelectrochemical cell. J Am Chem Soc, 2008, 130: 6342–6344
65 Sekizawa K, Maeda K, Domen K, Koike K, Ishitani O. Artificial Z-Scheme constructed with a supramolecular metal complex and semiconductor for the photocatalytic reduction of CO_2. J Am Chem Soc, 2013, 135: 4596–4599
66 Hara M, Nunoshige J, Takata T, Kondo JN, Domen K. Unusual enhancement of H_2 evolution by Ru on TaON photocatalyst under visible light irradiation. Chem Commun, 2003, 3000–3001
67 Kim ES, Nishimura N, Magesh G, *et al.* Fabrication of $CaFe_2O_4$/TaON heterojunction photoanode for photoelectrochemical water oxidation. J Am Chem Soc, 2013, 135: 5375–5383
68 Maeda K, Higashi M, Lu DL, Abe R, Domen K. Efficient nonsacrificial water splitting through two-step photoexcitation by visible light using a modified oxynitride as a hydrogen evolution photocatalyst. J Am Chem Soc, 2010, 132: 5858–5868
69 Mao J, Peng T, Zhang X, *et al.* Effect of graphitic carbon nitride microstructures on the activity and selectivity of photocatalytic CO_2 reduction under visible light. Catal Sci Technol, 2013, 3: 1253–1260
70 Wang X, Maeda K, Thomas A, *et al.* A metal-free polymeric photocatalyst for hydrogen production from water under visible light. Nat Mater, 2009, 8: 76–80
71 Zhang JS, Chen XF, Takanabe K, *et al.* Synthesis of a carbon nitride structure for visible-light catalysis by copolymerization. Angew Chem Int Ed, 2010, 49: 441–444
72 Kudo A, Ueda K, Kato H, Mikami I. Photocatalytic O_2 evolution under visible light irradiation on $BiVO_4$ in aqueous $AgNO_3$ solution. Catal Lett, 1998, 53: 229–230
73 Kudo A, Omori K, Kato H. A novel aqueous process for preparation of crystal form-controlled and highly crystalline $BiVO_4$ powder from layered vanadates at room temperature and its photocatalytic and photophysical properties. J Am Chem Soc, 1999, 121: 11459–11467
74 Tokunaga S, Kato H, Kudo A. Selective Preparation of monoclinic and tetragonal $BiVO_4$ with scheelite structure and their photocatalytic properties. Chem Mater, 2001, 13: 4624–4628
75 Jiang H, Dai H, Meng X, *et al.* Porous olive-like $BiVO_4$: alcoho-hydrothermal preparation and excellent visible-light-driven photocatalytic performance for the degradation of phenol. Appl Catal B-Environ, 2011, 105: 326–334
76 Jiang H, Meng X, Dai H, *et al.* High-performance porous spherical or octapod-like single-crystalline $BiVO_4$ photocatalysts for the removal of phenol and methylene blue under visible-light illumination. J Hazard Mater, 2012, 217–218: 92–99

77 Chun WJ, Ishikawa A, Fujisawa H, *et al.* Conduction and valence band positions of Ta_2O_5, TaON, and Ta_3N_5 by UPS and electrochemical methods. J Phys Chem B, 2003, 107: 1798–1803
78 Higashi M, Domen K, Abe R. Fabrication of efficient TaON and Ta_3N_5 photoanodes for water splitting under visible light irradiation. Energy Environ Sci, 2011, 4: 4138–4147
79 Li Y, Takata T, Cha D, *et al.* Vertically aligned Ta_3N_5 nanorod arrays for solar-driven photoelectrochemical water splitting. Adv Mater, 2012, 25: 125–131
80 Ma SSK, Hisatomi T, Maeda K, Moriya Y, Domen K. Enhanced water oxidation on Ta_3N_5 photocatalysts by modification with alkaline metal salts. J Am Chem Soc, 2012, 134: 19993–19996
81 He H, Zapol P, Curtiss LA. Computational screening of dopants for photocatalytic two-electron reduction of CO_2 on anatase (101) surfaces. Energy Environ Sci, 2012, 5: 6196–6205
82 Liu G, Hoivik N, Wang K, Jakobsen H. Engineering TiO_2 nanomaterials for CO_2 conversion/solar fuels. Sol Energ Mat Sol C, 2012, 105: 53–68
83 Sasirekha N, Basha SJS, Shanthi K. Photocatalytic performance of Ru doped anatase mounted on silica for reduction of carbon dioxide. Appl Catal B-Environ, 2006, 62: 169–180
84 Subrahmanyam M, Kaneco S, Alonso-Vante N. A screening for the photo reduction of carbon dioxide supported on metal oxide catalysts for C_1-C_3 selectivity. Appl Catal B-Environ, 1999, 23: 169–174
85 Pipornpong W, Wanbayor R, Ruangpornvisuti V. Adsorption CO_2 on the perfect and oxygen vacancy defect surfaces of anatase TiO_2 and its photocatalytic mechanism of conversion to CO. Appl Surf Sci, 2011, 257: 10322–10328
86 Anpo M, Yamashita H, Ichihashi Y, Ehara S. Photocatalytic reduction of CO_2 with H_2O on various titanium oxide catalysts. Electroanal Chem, 1995, 396: 21–26
87 Shkrob IA, Marin TW, He H, Zapol P. Photoredox reactions and the catalytic cycle for carbon dioxide fixation and methanogenesis on metal oxides. J Phys Chem C, 2012, 116: 9450–9460
88 Mori K, Yamashita H, Anpo M. Photocatalytic reduction of CO_2 with H_2O on various titanium oxide photocatalysts. RCS Advances, 2012, 2: 3165–3172
89 Wu JCS. Photocatalytic reduction of greenhouse gas CO_2 to fuel. Catal Surv Asia, 2009, 13: 30–40
90 Dimitrijevic NM, Vijayan BK, Poluektov OG, *et al.* Role of water and carbonates in photocatalytic transformation of CO_2 to CH_4 on titania. J Am Chem Soc, 2011, 133: 3964–3971
91 Yang CC, Vernimmen J, Meynen V, Cool P, Mul G. Mechanistic study of hydrocarbon formation in photocatalytic CO_2 reduction over Ti-SBA-15. J Catal, 2011, 284: 1–8
92 Ulagappan N, Frei H. Mechanistic study of CO_2 photoreduction in Ti silicalite molecular sieve by FT-IR spectroscopy. J Phys Chem A, 2000, 104: 7834–7839
93 Lin W, Han H, Frei H. CO_2 Splitting by H_2O to CO and O_2 under UV light in TiMCM-41 silicate sieve. J Phys Chem B, 2004, 108: 18269–18273
94 Chen J, Qin S, Song G, *et al.* Shape-controlled solvothermal synthesis of Bi2S3 for photocatalytic reduction of CO_2 to methyl formate in methanol. Dalton Trans, 2013, 42: 15133–15138
95 Qin SY, Xin F, Liu YD, Yin XH, Ma W. Photocatalytic reduction of CO_2 in methanol to Methyl formate over CuO-TiO_2 composite catalysts. J Colloid Interface Sci, 2011, 356: 257–261
96 Chen J, Xin F, Qin S, Yin X. Photocatalytically reducing CO_2 to methyl formate in methanol over ZnS and Ni-doped ZnS photocatalysts. Chem Eng J, 2013, 230: 506–512
97 Varghese OK, Paulose M, LaTempa TJ, Grimes CA. High-rate solar photocatalytic conversion of CO_2 and water vapor to hydrocarbon fuels. Nano Lett, 2010, 10: 750–750
98 Hoffmann MR, Moss JA, Baum MM. Artificial photosynthesis: semiconductor photocatalytic fixation of CO_2 to afford higher organic compounds. Dalton Trans, 2011, 40: 5151–5158
99 Schouten KJP, Kwon Y, van der Ham CJM, Qin Z, Koper MTM. A new mechanism for the selectivity to C_1 and C_2 species in the electrochemical reduction of carbon dioxide on copper electrodes. Chem Sci, 2011, 2: 1902–1909
100 Kocí K, Obalová L, Matejová L, *et al.* Effect of TiO_2 particle size on the photocatalytic reduction of CO_2. Appl Catal B-Environ, 2009, 89: 494–502
101 Kočí K, Matějů K, Obalová L, *et al.* Effect of silver doping on the TiO_2 for photocatalytic reduction of CO_2. Appl Catal B-Environ, 2010, 96: 239–244
102 Ku Y, Lee W, Wang W. Photocatalytic reduction of carbonate in aqueous solution by UV/TiO_2 process. J Mol Catal A-Chem, 2004, 212: 191–196
103 Tan SS, Zou L, Hu E. Kinetic modelling for photosynthesis of hydrogen and methane through catalytic reduction of carbon dioxide with water vapour. Catal Today, 2008, 131: 125–129
104 Lo CC, Hung CH, Yuan CS, Wu JF. Photoreduction of carbon dioxide with H_2 and H_2O over TiO_2 and ZrO_2 in a circulated photocatalytic reactor. Sol Energ Mat Sol C, 2007, 91: 1765–1774
105 Tahir M, Amin NS. Photocatalytic CO_2 reduction and kinetic study over In/TiO_2 NPs supported microchannel monolith photoreactor. Appl Catal A-Gen, 2013, 467: 483–496
106 Wasielewski MR. Self-assembly strategies for integrating light harvesting and charge separation in artificial photosynthetic systems. Acc Chem Res, 2009, 42: 1910–1921
107 Zhou H, Qu Y, Zeid T, Duan X. Towards highly efficient photocatalysts using semiconductor nanoarchitectures. Energy Environ Sci, 2012, 5: 6732–6743
108 Yu J, Jin J, Cheng B, Jaroniec M. A noble metal-free reduced graphene oxide-CdS nanorod composite for the enhanced visible-light photocatalytic reduction of CO_2 to solar fuel. J Mater Chem A, 2014, 2: 3407–3416
109 Lin J, Pan Z, Wang X. Photochemical reduction of CO_2 by graphitic carbon nitride polymers. ACS Sustain Chem Eng, 2013, 2: 353–358
110 Yu J, Wang K, Xiao W, Cheng B. Photocatalytic reduction of CO_2 into hydrocarbon solar fuels over g-C_3N_4-Pt nanocomposite photocatalysts. Phys Chem Chem Phys, 2014, 16: 11492–11501
111 Chen XY, Zhou Y, Liu Q, *et al.* Ultrathin, single-crystal WO_3 nanosheets by two-dimensional oriented attachment toward enhanced photocatalystic reduction of CO_2 into hydrocarbon fuels under visible light. ACS Appl Mater Interfaces, 2012, 4: 3372–3377
112 Xie YP, Liu G, Yin L, Cheng H-M. Crystal facet-dependent photocatalytic oxidation and reduction reactivity of monoclinic WO_3 for solar energy conversion. J Mater Chem, 2012, 22: 6746–6751
113 Matsumoto Y, Obata M, Hombo J. Photocatalytic reduction of carbon dioxide on *p*-type $CaFe_2O_4$ powder. J Phys Chem, 1994, 98: 2950–2951
114 Matsumoto Y. Energy positions of oxide semiconductors and photocatalysis with iron complex oxides. J Solid State Chem, 1996, 126: 227–234
115 Jia L, Li J, Fang W. Enhanced visible-light active C and Fe co-doped $LaCoO_3$ for reduction of carbon dioxide. Catal Commun, 2009, 11: 87–90
116 Liu YY, Huang BB, Dai Y, *et al.* Selective ethanol formation from photocatalytic reduction of carbon dioxide in water with $BiVO_4$ photocatalyst. Catal Commun, 2009, 11: 210–213
117 Mao J, Peng TY, Zhang XH, Li K, Zan L. Selective methanol production from photocatalytic reduction of CO_2 on $BiVO_4$ under visible light irradiation. Catal Commun, 2012, 28: 38–41
118 Zhou Y, Tian Z, Zhao Z, *et al.* High-yield synthesis of ultrathin and uniform Bi_2WO_6 square nanoplates benefitting from photocatalytic reduction of CO_2 into renewable hydrocarbon fuel under visible light. ACS Appl Mater Interfaces, 2011, 3: 3594–3601
119 Cheng H, Huang B, Liu Y, *et al.* An anion exchange approach to

Bi_2WO_6 hollow microspheres with efficient visible light photocatalytic reduction of CO_2 to methanol. Chem Commun, 2012, 48: 9729–9731
120 Li P, Zhou Y, Tu WG, *et al.* Direct growth of $Fe_2V_4O_{13}$ nanoribbons on a stainless-steel mesh for visible-light photoreduction of CO_2 into renewable hydrocarbon fuel and degradation of gaseous isopropyl alcohol. ChemPlusChem, 2013, 78: 274–278
121 Wang ZY, Chou HC, Wu JCS, Tsai DP, Mul G. CO_2 photoreduction using NiO/$InTaO_4$ in optical-fiber reactor for renewable energy. Appl Catal A-Gen, 2010, 380: 172–177
122 Pan PW, Chen YW. Photocatalytic reduction of carbon dioxide on NiO/$InTaO_4$ under visible light irradiation. Catal Commun, 2007, 8: 1546–1549
123 Chen HC, Chou HC, Wu JCS, Lin HY. Sol-gel prepared $InTaO_4$ and its photocatalytic characteristics. J Mater Res, 2008, 23: 1364–1370
124 Tsai C-W, Chen HM, Liu R-S, Asakura K, Chan T-S. Ni@NiO core–shell structure-modified nitrogen-doped $InTaO_4$ for solar-driven highly efficient CO_2 reduction to methanol. J Phys Chem C, 2011, 115: 10180–10186
125 Serpone N, Emeline AV. Semiconductor photocatalysis—Past, present, and future outlook. J Phys Chem Lett, 2012, 3: 673–677
126 Serpone N. Is the band gap of pristine TiO_2 narrowed by anion- and cation-doping of titanium dioxide in second-generation photocatalysts? J Phys Chem B, 2006, 110: 24287–24293
127 Li XK, Zhuang ZJ, Li W, Pan HQ. Photocatalytic reduction of CO_2 over noble metal-loaded and nitrogen-doped mesoporous TiO_2. Appl Catal A-Gen, 2012, 429: 31–38
128 Suzuki TM, Nakamura T, Saeki S, *et al.* Visible light-sensitive mesoporous N-doped Ta_2O_5 spheres: synthesis and photocatalytic activity for hydrogen evolution and CO_2 reduction. J Mater Chem, 2012, 22: 24584–24590
129 Zhang QY, Li Y, Ackerman EA, Gajdardziska-Josifovska M, Li HL. Visible light responsive iodine-doped TiO_2 for photocatalytic reduction of CO_2 to fuels. Appl Catal A-Gen, 2011, 400: 195–202
130 Zhang QY, Gao TT, Andino JM, Li Y. Copper and iodine co-modified TiO_2 NPs for improved activity of CO_2 photoreduction with water vapor. Appl Catal B-Environ, 2012, 123: 257–264
131 Slamet, Nasution HW, Purnama E, Kosela S, Gunlazuardi J. Photocatalytic reduction of CO_2 on copper-doped titania catalysts prepared by improved-impregnation method. Catal Commun, 2005, 6: 313–319
132 Tseng IH, Wu JCS. Chemical states of metal-loaded titania in the photoreduction of CO_2. Catal Today, 2004, 97: 113–119
133 Tseng IH, Wu JCS, Chou HY. Effects of sol-gel procedures on the photocatalysis of Cu/TiO_2 in CO_2 photoreduction. J Catal, 2004, 221: 432–440
134 Luo DM, Bi Y, Kan W, Zhang N, Hong SG. Copper and cerium co-doped titanium dioxide on catalytic photo reduction of carbon dioxide with water: experimental and theoretical studies. J Mol Struct, 2011, 994: 325–331
135 Richardson PL, Perdigoto MLN, Wang W, Lopes RJG. Manganese- and copper-doped titania nanocomposites for the photocatalytic reduction of carbon dioxide into methanol. Appl Catal B-Environ, 2012, 126: 200–207
136 Ishitani O, Inoue C, Suzuki Y, Ibusuki T. Photocatalytic reduction of carbon dioxide to methane and acetic acid by an aqueous suspension of metal-deposited TiO_2. J Photoch Photobio A, 1993, 72: 269–271
137 Fan J, Liu EZ, Tian L, *et al.* Synergistic effect of N and Ni^{2+} on nanotitania in photocatalytic reduction of CO_2. J Environ Eng-Asce, 2011, 137: 171–176
138 Hou WB, Hung WH, Pavaskar P, *et al.* Photocatalytic conversion of CO_2 to hydrocarbon fuels via plasmon-enhanced absorption and metallic interband transitions. ACS Catal, 2011, 1: 929–936
139 Manzanares M, Fabrega C, Osso JO, *et al.* Engineering the TiO_2 outermost layers using magnesium for carbon dioxide photoreduction. Appl Catal B-Environ, 2014, 150: 57–62
140 Zuo F, Wang L, Wu T, *et al.* Self-doped Ti^{3+} enhanced photocatalyst for hydrogen production under visible light. J Am Chem Soc, 2010, 132: 11856–11857
141 Xi G, Ouyang S, Li P, *et al.* Ultrathin $W_{18}O_{49}$ nanowires with diameters below 1 nm: synthesis, near-infrared absorption, photoluminescence, and photochemical reduction of carbon dioxide. Angew Chem Int Ed, 2012, 51: 2395–2399
142 Pan X, Yang M-Q, Fu X, Zhang N, Xu Y-J. Defective TiO_2 with oxygen vacancies: synthesis, properties and photocatalytic applications. Nanoscale, 2013, 5: 3601–3614
143 Liu L, Zhao H, Andino JM, Li Y. Photocatalytic CO_2 reduction with H_2O on TiO_2 nanocrystals: comparison of anatase, rutile, and brookite polymorphs and exploration of surface chemistry. ACS Catal, 2012, 2: 1817–1828
144 Liu LJ, Gao F, Zhao HL, Li Y. Tailoring Cu valence and oxygen vacancy in Cu/TiO_2 catalysts for enhanced CO_2 photoreduction efficiency. Appl Catal B-Environ, 2013, 134: 349–358
145 Li P, Zhou Y, Tu W, *et al.* Synthesis of $Bi_6Mo_2O_{15}$ sub-microwires via a molten salt method and enhancing the photocatalytic reduction of CO_2 into solar fuel through tuning the surface oxide vacancies by simple post-heating treatment. CrystEngComm, 2013, 15: 9855–9858
146 Jiang D, Wang WZ, Gao EP, Sun SM, Zhang L. Highly selective defect-mediated photochemical CO_2 conversion over fluorite ceria under ambient conditions. Chem Commun, 2014, 50: 2005–2007
147 Kong M, Li Y, Chen X, *et al.* Tuning the relative concentration ratio of bulk defects to surface defects in TiO_2 nanocrystals leads to high photocatalytic efficiency. J Am Chem Soc, 2011, 133: 16414–16417
148 Zhuang J, Dai W, Tian Q, *et al.* Photocatalytic degradation of RhB over TiO_2 bilayer films: effect of defects and their location. Langmuir, 2010, 26: 9686–9694
149 Zhao Z, Fan J, Liu S, Wang Z. Optimal design and preparation of titania-supported CoPc using sol-gel for the photo-reduction of CO_2. Chem Eng J, 2009, 151: 134–140
150 Zhao ZH, Fan JM, Xie MM, Wang ZZ. Photo-catalytic reduction of carbon dioxide with *in-situ* synthesized CoPc/TiO_2 under visible light irradiation. J Clean Prod, 2009, 17: 1025–1029
151 Zhao ZH, Fan JM, Wang ZZ. Photo-catalytic CO_2 reduction using sol-gel derived titania-supported zinc-phthalocyanine. J Clean Prod, 2007, 15: 1894–1897
152 Kumar P, Kumar A, Sreedhar B, *et al.* Cobalt phthalocyanine immobilized on graphene oxide: an efficient visible-active catalyst for the photoreduction of carbon dioxide. Chem-Eur J, 2014, 20: 6154–6161
153 Yuan YJ, Yu ZT, Zhang JY, Zou ZG. A copper(I) dye-sensitised TiO_2-based system for efficient light harvesting and photoconversion of CO2 into hydrocarbon fuel. Dalton Trans, 2012, 41: 9594–9597
154 Nguyen TV, Wu JCS, Chiou CH. Photoreduction of CO_2 over Ruthenium dye-sensitized TiO_2-based catalysts under concentrated natural sunlight. Catal Commun, 2008, 9: 2073–2076
155 Wang C, Thompson RL, Baltrus J, Matranga C. Visible light photoreduction of CO_2 using CdSe/Pt/TiO_2 heterostructured catalysts. J Phys Chem Lett, 2009, 1: 48–53
156 Wang CJ, Thompson RL, Ohodnicki P, Baltrus J, Matrang C. Size-dependent photocatalytic reduction of CO_2 with PbS quantum dot sensitized TiO_2 heterostructured photocatalysts. J Mater Chem, 2011, 21: 13452–13457
157 Abou Asi M, He C, Su MH, *et al.* Photocatalytic reduction of CO_2 to hydrocarbons using AgBr/TiO_2 nanocomposites under visible light. Catal Today, 2011, 175: 256–263
158 Singh V, Beltran IJC, Ribot JC, Nagpal P. Photocatalysis deconstructed: design of a new selective catalyst for artificial photosynthesis. Nano Lett, 2014, 14: 597–603

159 Li H, He X, Kang Z, *et al.* Water-soluble fluorescent carbon quantum dots and photocatalyst design. Angew Chem Int Ed, 2010, 49: 4430–4434
160 Zhang H, Ming H, Lian S, *et al.* Fe_2O_3/carbon quantum dots complex photocatalysts and their enhanced photocatalytic activity under visible light. Dalton Trans, 2011, 40: 10822–10825
161 Kang Z, Tsang CHA, Wong N-B, Zhang Z, Lee S-T. Silicon quantum dots: a general photocatalyst for reduction, decomposition, and selective oxidation reactions. J Am Chem Soc, 2007, 129: 12090–12091
162 Li Q, Cui C, Meng H, Yu J. Visible-light photocatalytic hydrogen production activity of $ZnIn_2S_4$ microspheres using carbon quantum dots and platinum as dual co-catalysts. Chem Asian J, 2014, 9: 1766–1770
163 Linic S, Christopher P, Ingram DB. Plasmonic-metal nanostructures for efficient conversion of solar to chemical energy. Nat Mater, 2011, 10: 911–921
164 Zhang Z, Wang Z, Cao S-W, Xue C. Au/Pt nanoparticle-decorated TiO_2 nanofibers with plasmon-enhanced photocatalytic activities for solar-to-fuel conversion. J Phys Chem C, 2013, 117: 25939–25947
165 Liu E, Hu Y, Li H, *et al.* Photoconversion of CO_2 to methanol over plasmonic Ag/TiO_2 nano-wire films enhanced by overlapped visible-light-harvesting nanostructures. Ceram Int, 2015, 41: 1049–1057
166 An C, Wang J, Jiang W, *et al.* Strongly visible-light responsive plasmonic shaped AgX:Ag (X = Cl, Br) NPs for reduction of CO_2 to methanol. Nanoscale, 2012, 4: 5646–5650
167 Liu E, Kang L, Wu F, *et al.* Photocatalytic reduction of CO_2 into methanol over Ag/TiO_2 nanocomposites enhanced by surface plasmon resonance. Plasmonics, 2013, 9: 1–10
168 Kong D, Tan JZY, Yang F, Zeng J, Zhang X. Electrodeposited Ag NPs on TiO_2 nanorods for enhanced UV visible light photoreduction CO_2 to CH_4. Appl Surf Sci, 2013, 277: 105–110
169 Tan JZY, Fernandez Y, Liu D, *et al.* Photoreduction of CO_2 using copper-decorated TiO_2 nanorod films with localized surface plasmon behavior. Chem Phys Lett, 2012, 531: 149–154
170 Cortie MB, McDonagh AM. Synthesis and optical properties of hybrid and alloy plasmonic NPs. Chem Rev, 2011, 111: 3713–3735
171 Chan GH, Zhao J, Hicks EM, Schatz GC, Van Duyne RP. Plasmonic properties of copper NPs fabricated by nanosphere lithography. Nano Lett, 2007, 7: 1947–1952
172 Ovcharov ML, Shvalagin VV, Granchak VM. Photocatalytic reduction of CO_2 on mesoporous TiO_2 modified with Ag/Cu bimetallic nanostructures. Theor Exp Chem, 2014, 50: 175–180
173 Neaţu Ş, Maciá-Agulló JA, Concepción P, Garcia H. Gold-copper nanoalloys supported on TiO_2 as photocatalysts for CO_2 reduction by water. J Am Chem Soc, 2014, 136: 15969–15976
174 Lekse JW, Underwood MK, Lewis JP, Matranga C. Synthesis, characterization, electronic structure, and photocatalytic behavior of $CuGaO_2$ and $CuGa_{1-x}Fe_xO_2$ (x = 0.05, 0.10, 0.15, 0.20) delafossites. J Phys Chem C, 2011, 116: 1865–1872
175 Liu JY, Garg B, Ling YC. CuxAgyInzZnkSm solid solutions customized with RuO_2 or $Rh_{1.32}Cr_{0.66}O_3$ co-catalyst display visible light-driven catalytic activity for CO_2 reduction to CH_3OH. Green Chem, 2011, 13: 2029–2031
176 Zhang N, Ouyang S, Kako T, Ye J. Mesoporous zinc germanium oxynitride for CO_2 photoreduction under visible light. Chem Commun, 2012, 48: 1269–1271
177 Liu Q, Zhou Y, Tian ZP, *et al.* Zn_2GeO_4 crystal splitting toward sheaf-like, hyperbranched nanostructures and photocatalytic reduction of CO_2 into CH_4 under visible light after nitridation. J Mater Chem, 2012, 22: 2033–2038
178 Yan S, Yu H, Wang N, Li Z, Zou Z. Efficient conversion of CO_2 and H_2O into hydrocarbon fuel over $ZnAl_2O_4$-modified mesoporous ZnGaNO under visible light irradiation. Chem Commun, 2012, 48: 1048–1050
179 Yan S, Wang J, Gao H, *et al.* Zinc gallogermanate solid solution: a novel photocatalyst for efficiently converting CO_2 into solar fuels. Adv Funct Mater, 2013, 23: 1839–1845
180 Chen X, Li C, Gratzel M, Kostecki R, Mao SS. Nanomaterials for renewable energy production and storage. Chem Soc Rev, 2012, 41: 7909–7937
181 Liu BJ, Torimoto T, Matsumoto H, Yoneyama H. Effect of solvents on photocatalytic reduction of carbon dioxide using TiO_2 nanocrystal photocatalyst embedded in SiO_2 matrices. J Photoch Photobio A, 1997, 108: 187–192
182 Liu BJ, Torimoto T, Yoneyama H. Photocatalytic reduction of carbon dioxide in the presence of nitrate using TiO_2 nanocrystal photocatalyst embedded in SiO_2 matrices. J Photoch Photobio A, 1998, 115: 227–230
183 Koci K, Obalova L, Placha D, Lacny Z. Effect of temperature, pressure and volume of reacting phase on photocatalytic CO_2 reduction on suspended nanocrystalline TiO_2. Collect Czech Chem C, 2008, 73: 1192–1204
184 Yanagida S, Wada Y, Murakoshi K, *et al.* Photocatalytic reduction and fixation of CO_2 on cadmium sulfide nanocrystallites. In: Inui T, Anpo M, Izui K, Yanagida S and Yamaguchi T (eds.). Advances in Chemical Conversions for Mitigating Carbon Dioxide, Proceedings of the Fourth International Conference on Carbon Dioxide Utilization. Amsterdam: Elsevier, 1998, 114: 183–188
185 Peng F, Wang J, Ge GL, *et al.* Photochemical reduction of CO_2 catalyzed by silicon nanocrystals produced by high energy ball milling. Mater Lett, 2013, 92: 65–67
186 Feng XJ, Sloppy JD, LaTemp TJ, *et al.* Synthesis and deposition of ultrafine Pt NPs within high aspect ratio TiO_2 nanotube arrays: application to the photocatalytic reduction of carbon dioxide. J Mater Chem, 2011, 21: 13429–13433
187 Zhang QH, Han WD, Hong YJ, Yu JG. Photocatalytic reduction of CO_2 with H_2O on Pt-loaded TiO_2 catalyst. Catal Today, 2009, 148: 335–340
188 Zhang XJ, Han F, Shi B, *et al.* Photocatalytic conversion of diluted CO_2 into light hydrocarbons using periodically modulated multiwalled nanotube arrays. Angew Chem Int Ed, 2012, 51: 12732–12735
189 Raja KSRKS, Smith YR, Kondamudi N, *et al.* CO_2 photoreduction in the liquid phase over Pd-supported on TiO_2 nanotube and bismuth titanate photocatalysts. Electrochem Solid-State Lett, 2011, 14: F5–F8
190 Zhao ZH, Fan JM, Wang JY, Li RF. Effect of heating temperature on photocatalytic reduction of CO_2 by N-TiO_2 nanotube catalyst. Catal Commun, 2012, 21: 32–37
191 Vijayan B, Dimitrijevic NM, Rajh T, Gray K. Effect of calcination temperature on the photocatalytic reduction and oxidation processes of hydrothermally synthesized titania nanotubes. J Phys Chem C, 2010, 114: 12994–13002
192 Fu J, Cao S, Yu J, Low J, Lei Y. Enhanced photocatalytic CO_2-reduction activity of electrospun mesoporous TiO_2 nanofibers by solvothermal treatment. Dalton Trans, 2014, 43: 9158–9165
193 Wang PQ, Bai Y, Liu JY, Fan Z, Hu YQ. One-pot synthesis of rutile TiO_2 nanoparticle modified anatase TiO_2 nanorods toward enhanced photocatalytic reduction of CO_2 into hydrocarbon fuels. Catal Commun, 2012, 29: 185–188
194 Shi HF, Wang TZ, Chen J, *et al.* Photoreduction of carbon dioxide over $NaNbO_3$ nanostructured photocatalysts. Catal Lett, 2011, 141: 525–530
195 Liu Q, Zhou Y, Kou JH, *et al.* High-yield synthesis of ultralong and ultrathin Zn_2GeO_4 nanoribbons toward improved photocatalytic reduction of CO_2 into renewable hydrocarbon fuel. J Am Chem Soc, 2010, 132: 14385–14387

196 Yan SC, Wan LJ, Li ZS, Zou ZG. Facile temperature-controlled synthesis of hexagonal Zn_2GeO_4 nanorods with different aspect ratios toward improved photocatalytic activity for overall water splitting and photoreduction of CO_2. Chem Commun, 2011, 47: 5632–5634

197 Li XK, Pan HQ, Li W, Zhuang ZJ. Photocatalytic reduction of CO_2 to methane over HNb_3O_8 nanobelts. Appl Catal A-Gen, 2012, 413: 103–108

198 Xu H, Ouyang SX, Li P, Kako T, Ye JH. High-active anatase TiO_2 nanosheets exposed with 95% {100} facets toward efficient H_2 evolution and CO_2 photoreduction. ACS Appl Mater Interfaces, 2013, 5: 1348–1354

199 Jiao W, Wang L, Liu G, Lu GQ, Cheng H-M. Hollow anatase TiO_2 single crystals and mesocrystals with dominant {101} facets for improved photocatalysis activity and tuned reaction preference. ACS Catal, 2012, 2: 1854–1859

200 Mao J, Ye L, Li K, *et al.* Pt-loading reverses the photocatalytic activity order of anatase TiO_2 {001} and {010} facets for photoreduction of CO_2 to CH_4. Appl Catal B-Environ, 2014, 144: 855–862

201 Yu J, Low J, Xiao W, Zhou P, Jaroniec M. Enhanced photocatalytic CO_2-reduction activity of anatase TiO_2 by coexposed {001} and {101} facets. J Am Chem Soc, 2014, 136: 8839–8842

202 Yan S, Wang J, Gao H, *et al.* An ion-exchange phase transformation to $ZnGa_2O_4$ nanocube towards efficient solar fuel synthesis. Adv Funct Mater, 2013, 23: 758–763

203 Liu Q, Wu D, Zhou Y, *et al.* Single-crystalline, ultrathin $ZnGa_2O_4$ nanosheet scaffolds to promote photocatalytic activity in CO_2 reduction into methane. ACS Appl Mater Interfaces, 2014, 6: 2356–2361

204 Zhang L, Wang W, Jiang D, Gao E, Sun S. Photoreduction of CO_2 on BiOCl nanoplates with the assistance of photoinduced oxygen vacancies. Nano Res, doi: 10.1007/s12274-014-0564-2

205 Li Z, Zhou Y, Zhang J, *et al.* Hexagonal nanoplate-textured micro-octahedron Zn_2SnO_4: combined effects toward enhanced efficiencies of dye-sensitized solar cell and photoreduction of CO_2 into hydrocarbon fuels. Cryst Growth Des, 2012, 12: 1476–1481

206 Nicolosi V, Chhowalla M, Kanatzidis MG, Strano MS, Coleman JN. Liquid exfoliation of layered materials. Science, 2013, 340: 1420

207 Jiao J, Wei Y, Zhao Z, *et al.* Photocatalysts of 3D ordered macroporous TiO_2-supported CeO_2 nanolayers: design, preparation, and their catalytic performances for the reduction of CO_2 with H_2O under simulated solar irradiation. Ind Eng Chem Res, 2014, 53: 17345–14754

208 Truong QD, Le TH, Liu JY, Chung CC, Ling YC. Synthesis of TiO_2 NPs using novel titanium oxalate complex towards visible light-driven photocatalytic reduction of CO_2 to CH_3OH. Appl Catal A-Gen, 2012, 437: 28–35

209 Zhao HL, Liu LJ, Andino JM, Li Y. Bicrystalline TiO_2 with controllable anatase-brookite phase content for enhanced CO_2 photoreduction to fuels. J Mater Chem A, 2013, 1: 8209–8216

210 Chen L, Graham ME, Li GH, *et al.* Photoreduction of CO_2 by TiO_2 nanocomposites synthesized through reactive direct current magnetron sputter deposition. Thin Solid Films, 2009, 517: 5641–5645

211 Li G, Ciston S, Saponjic ZV, *et al.* Synthesizing mixed-phase TiO_2 nanocomposites using a hydrothermal method for photo-oxidation and photoreduction applications. J Catal, 2008, 253: 105–110

212 Li P, Xu H, Liu L, *et al.* Constructing cubic-orthorhombic surface-phase junctions of $NaNbO_3$ towards significant enhancement of CO_2 photoreduction. J Mater Chem A, 2014, 2: 5606–5609

213 Liu M, Jing D, Zhou Z, Guo L. Twin-induced one-dimensional photocatalytic and photoelectrochemical applicationsions yield high quantum efficiency for solar hydrogen generation. Nat Commun, 2013, 4: 2278

214 Abdi FF, Han L, Smets AHM, *et al.* Efficient solar water splitting by enhanced charge separation in a bismuth vanadate-silicon tandem photoelectrode. Nat Commun, 2013, 4: 2195

215 Sun YY, Wang WZ, Zhang L, Zhang ZJ. Design and controllable synthesis of alpha-/gamma-Bi_2O_3 homojunction with synergetic effect on photocatalytic activity. Chem Eng J, 2012, 211: 161–167

216 McShane CM, Siripala WP, Choi K-S. Effect of junction morphology on the performance of polycrystalline Cu_2O homojunction solar cells. J Phys Chem Lett, 2010, 1: 2666–2670

217 Wang YG, Li B, Zhang CL, *et al.* Ordered mesoporous CeO_2-TiO_2 composites: highly efficient photocatalysts for the reduction of CO_2 with H_2O under simulated solar irradiation. Appl Catal B-Environ, 2013, 130: 277–284

218 In SI, Vaughn DD, Schaak RE. Hybrid CuO-$TiO_{2-x}N_x$ hollow nanocubes for photocatalytic conversion of CO_2 into methane under solar irradiation. Angew Chem Int Edit, 2012, 51: 3915–3918

219 Cao S-W, Liu X-F, Yuan Y-P, *et al.* Solar-to-fuels conversion over In_2O_3/g-C_3N_4 hybrid photocatalysts. Appl Catal B-Environ, 2014, 147: 940–946

220 Pan CS, Xu J, Wang YJ, Li D, Zhu YF. Dramatic activity of C_3N_4/$BiPO_4$ photocatalyst with core/shell structure formed by self-assembly. Adv Funct Mater, 2012, 22: 1518–1524

221 Hwang YJ, Boukai A, Yang P. High density *n*-Si/*n*-TiO_2 core/shell nanowire arrays with enhanced photoactivity. Nano Lett, 2008, 9: 410–415

222 Hou Y, Zuo F, Dagg A, Feng P. Visible light-driven α-Fe_2O_3 nanorod/graphene/$BiV_{1-x}Mo_xO_4$ core/shell heterojunction array for efficient photoelectrochemical water splitting. Nano Lett, 2012, 12: 6464–6473

223 Low J, Cao S, Yu J, Wageh S. Two-dimensional layered composite photocatalysts. Chem Commun, 2014, 50: 10768–10777

224 Woan K, Pyrgiotakis G, Sigmund W. Photocatalytic carbon-nanotube-TiO_2 composites. Adv Mater, 2009, 21: 2233–2239

225 Fan WQ, Zhang QH, Wang Y. Semiconductor-based nanocomposites for photocatalytic H_2 production and CO_2 conversion. Phys Chem Chem Phys, 2013, 15: 2632–2649

226 Leary R, Westwood A. Carbonaceous nanomaterials for the enhancement of TiO_2 photocatalysis. Carbon, 2011, 49: 741–772

227 Yu J, Ma T, Liu S. Enhanced photocatalytic activity of mesoporous TiO_2 aggregates by embedding carbon nanotubes as electron-transfer channel. Phys Chem Chem Phys, 2011, 13: 3491–3501

228 Yu J, Yang B, Cheng B. Noble-metal-free carbon nanotube-$Cd_{0.1}Zn_{0.9}S$ composites for high visible-light photocatalytic H_2-production performance. Nanoscale, 2012, 4: 2670–2677

229 Xia X-H, Jia Z-J, Yu Y, *et al.* Preparation of multi-walled carbon nanotube supported TiO_2 and its photocatalytic activity in the reduction of CO_2 with H_2O. Carbon, 2007, 45: 717–721

230 Ong WJ, Gui MM, Chai SP, Mohamed AR. Direct growth of carbon nanotubes on Ni/TiO_2 as next generation catalysts for photoreduction of CO_2 to methane by water under visible light irradiation. RSC Adv, 2013, 3: 4505–4509

231 Gui MM, Chai S-P, Xu B-Q, Mohamed AR. Enhanced visible light responsive MWCNT/TiO_2 core-shell nanocomposites as the potential photocatalyst for reduction of CO_2 into methane. Sol Energ Mat Sol C, 2014, 122: 183–189

232 Xiang QJ, Yu JG, Jaroniec M. Graphene-based semiconductor photocatalysts. Chem Soc Rev, 2012, 41: 782–796

233 Xiang Q, Yu J. Graphene-based photocatalysts for hydrogen generation. J Phys Chem Lett, 2013, 4: 753–759

234 Xie G, Zhang K, Guo B, *et al.* Graphene-based materials for hydrogen generation from light-driven water splitting. Adv Mater, 2013, 25: 3820–3839

235 Lightcap IV, Kosel TH, Kamat PV. Anchoring semiconductor and metal NPs on a two-dimensional catalyst mat. Storing and shuttling electrons with reduced graphene oxide. Nano Lett, 2010, 10: 577–583

236 Williams G, Seger B, Kamat PV. TiO_2-graphene nanocomposites. UV-assisted photocatalytic reduction of graphene oxide. ACS

Nano, 2008, 2: 1487–1491
237 Xiang Q, Yu J, Jaroniec M. Synergetic effect of MoS_2 and graphene as co-catalysts for enhanced photocatalytic H_2 production activity of TiO_2 NPs. J Am Chem Soc, 2012, 134: 6575–6578
238 Zhang J, Yu J, Jaroniec M, Gong JR. Noble metal-free reduced graphene oxide-$Zn_xCd_{1-x}S$ nanocomposite with enhanced solar photocatalytic H_2-production performance. Nano Lett, 2012, 12: 4584–4589
239 Zhang J, Qi L, Ran J, Yu J, Qiao SZ. Ternary NiS/$Zn_xCd_{1-x}S$/reduced graphene oxide nanocomposites for enhanced solar photocatalytic H_2-production activity. Adv Energy Mater, 2014, 4: 1301925
240 Wang Y, Yu J, Xiao W, Li Q. Microwave-assisted hydrothermal synthesis of graphene based Au-TiO_2 photocatalysts for efficient visible-light hydrogen production. J Mater Chem A, 2014, 2: 3847–3855
241 Hsu HC, Shown I, Wei HY, *et al.* Graphene oxide as a promising photocatalyst for CO_2 to methanol conversion. Nanoscale, 2013, 5: 262–268
242 Liang YT, Vijayan BK, Gray KA, Hersam MC. Minimizing graphene defects enhances titania nanocomposite-based photocatalytic reduction of CO_2 for improved solar fuel production. Nano Lett, 2011, 11: 2865–2870
243 Tu WG, Zhou Y, Liu Q, *et al.* Robust hollow spheres consisting of alternating titania nanosheets and graphene nanosheets with high photocatalytic activity for CO_2 conversion into renewable fuels. Adv Funct Mater, 2012, 22: 1215–1221
244 Tu WG, Zhou Y, Liu Q, *et al.* An in situ simultaneous reduction-hydrolysis technique for fabrication of TiO_2-graphene 2D sandwich-like hybrid nanosheets: graphene-promoted selectivity of photocatalytic-driven hydrogenation and coupling of CO_2 into methane and ethane. Adv Funct Mater, 2013, 23: 1743–1749
245 Wang Y, Chen Y, Zuo Y, *et al.* Hierarchically mesostructured TiO_2/graphitic carbon composite as a new efficient photocatalyst for the reduction of CO_2 under simulated solar irradiation. Catal Sci Technol, 2013, 3: 3286–3291
246 Lv XJ, Fu WF, Hu CY, Chen Y, Zhou WB. Photocatalytic reduction of CO_2 with H_2O over a graphene-modified NiO_x-Ta_2O_5 composite photocatalyst: coupling yields of methanol and hydrogen. RSC Adv, 2013, 3: 1753–1757
247 Wang PQ, Bai Y, Luo PY, Liu JY. Graphene-WO_3 nanobelt composite: elevated conduction band toward photocatalytic reduction of CO_2 into hydrocarbon fuels. Catal Commun, 2013, 38: 82–85
248 An X, Li K, Tang J. Cu_2O/reduced graphene oxide composites for the photocatalytic conversion of CO_2. ChemSusChem, 2014, 7: 1086–1093
249 Indrakanti VP, Schobert HH, Kubicki JD. Quantum mechanical modeling of CO_2 interactions with irradiated stoichiometric and oxygen-deficient anatase TiO_2 surfaces: implications for the photocatalytic reduction of CO_2. Energ Fuel, 2009, 23: 5247–5256
250 He H, Zapol P, Curtiss LA. A theoretical study of CO_2 anions on anatase (101) surface. J Phys Chem C, 2010, 114: 21474–21481
251 Rasko J, Solymosi F. Infrared spectroscopic study of the photoinduced activation of CO_2 on TiO_2 and Rh/TiO_2 catalysts. J Phys Chem, 1994, 98: 7147–7152
252 Finkelstein-Shapiro D, Petrosko SH, Dimitrijevic NM, *et al.* CO_2 preactivation in photoinduced reduction via surface functionalization of TiO_2 NPs. J Phys Chem Lett, 2013, 4: 475–479
253 Lee D, Kanai Y. Role of four-fold coordinated titanium and quantum confinement in CO_2 reduction at titania surface. J Am Chem Soc, 2012, 134: 20266–20269
254 Michalkiewicz B, Majewska J, Kądziołka G, *et al.* Reduction of CO_2 by adsorption and reaction on surface of TiO_2-nitrogen modified photocatalyst. J CO_2 Util, 2014, 5: 47–52
255 Sumida K, Rogow DL, Mason JA, *et al.* Carbon dioxide capture in metal-organic frameworks. Chem Rev, 2012, 112: 724–781
256 Li JR, Kuppler RJ, Zhou HC. Selective gas adsorption and separation in metal-organic frameworks. Chem Soc Rev, 2009, 38: 1477–1504
257 Silva CG, Corma A, Garcia H. Metal-organic frameworks as semiconductors. J Mater Chem, 2010, 20: 3141–3156
258 Wang D, Huang R, Liu W, Sun D, Li Z. Fe-based MOFs for photocatalytic CO_2 reduction: role of coordination unsaturated sites and dual excitation pathways. ACS Catal, 2014, 4: 4254–4260
259 Fu YH, Sun DR, Chen YJ, *et al.* An amine-functionalized titanium metal-organic framework photocatalyst with visible-light-induced activity for CO_2 reduction. Angew Chem Int Ed, 2012, 51: 3364–3367
260 Wang C, Xie Z, deKrafft KE, Lin W. Doping metal-organic frameworks for water oxidation, carbon dioxide reduction, and organic photocatalysis. J Am Chem Soc, 2011, 133: 13445–13454
261 Li J, Luo D, Yang C, *et al.* Copper(II) imidazolate frameworks as highly efficient photocatalysts for reduction of CO_2 into methanol under visible light irradiation. J Solid State Chem, 2013, 203: 154–159
262 Wang S, Yao W, Lin J, Ding Z, Wang X. Cobalt imidazolate metal-organic frameworks photosplit CO_2 under mild reaction conditions. Angew Chem Int Ed, 2014, 53: 1034–1038
263 Wang S, Wang X. Photocatalytic CO_2 reduction by CdS promoted with a zeolitic imidazolate framework. Appl Catal B-Environ, 2015, 162: 494–500
264 Liu Q, Low ZX, Li LX, *et al.* ZIF-8/Zn_2GeO_4 nanorods with an enhanced CO_2 adsorption property in an aqueous medium for photocatalytic synthesis of liquid fuel. J Mater Chem A, 2013, 1: 11563–11569
265 Wang J, Senkovska I, Oschatz M, *et al.* Imine-linked polymer-derived nitrogen-doped microporous carbons with excellent CO_2 capture properties. ACS Appl Mater Interfaces, 2013, 5: 3160–3167
266 Liao Y, Cao S-W, Yuan Y, *et al.* Efficient CO_2 capture and photoreduction by amine-functionalized TiO_2. Chem-Eur J, 2014, 20: 10220–10222
267 Shi H, Chen G, Zhang C, Zou Z. Polymeric g-C_3N_4 coupled with $NaNbO_3$ nanowires toward enhanced photocatalytic reduction of CO_2 into renewable fuel. ACS Catal, 2014, 4: 3637–3643
268 Zhao Y, Yang L, Chen S, *et al.* Can boron and nitrogen co-doping improve oxygen reduction reaction activity of carbon nanotubes? J Am Chem Soc, 2013, 135: 1201–1204
269 Zhao Y, Nakamura R, Kamiya K, Nakanishi S, Hashimoto K. Nitrogen-doped carbon nanomaterials as non-metal electrocatalysts for water oxidation. Nat Commun, 2013, 4: 2390
270 Gong KP, Du F, Xia ZH, Durstock M, Dai LM. Nitrogen-doped carbon nanotube arrays with high electrocatalytic activity for oxygen reduction. Science, 2009, 323: 760–764
271 Meng X, Ouyang S, Kako T, *et al.* Photocatalytic CO_2 reduction into CH_4 over alkali modified TiO_2 without noble metal co-catalysts loaded. Chem Commun, 2014, 50: 11517–11519
272 Teramura K, Tanaka T, Ishikawa H, Kohno Y, Funabiki T. Photocatalytic reduction of CO_2 to CO in the presence of H_2 or CH_4 as a reductant over MgO. J Phys Chem B, 2004, 108: 346–354
273 Kohno Y, Ishikawa H, Tanaka T, Funabiki T, Yoshida S. Photoreduction of carbon dioxide by hydrogen over magnesium oxide. Phys Chem Chem Phys, 2001, 3: 1108–1113
274 Kohno Y, Tanaka T, Funabiki T, Yoshida S. Reaction mechanism in the photoreduction of CO_2 with CH_4 over ZrO_2 Phys Chem Chem Phys, 2000, 2: 5302–5307
275 Liu L, Zhao C, Zhao H, Pitts D, Li Y. Porous microspheres of MgO-patched TiO_2 for CO_2 photoreduction with H_2O vapor: temperature-dependent activity and stability. Chem Commun, 2013, 49: 3664–3666
276 Xie S, Wang Y, Zhang Q, *et al.* Photocatalytic reduction of CO_2 with H_2O: significant enhancement of the activity of Pt-TiO_2 in CH_4 formation by addition of MgO. Chem Commun, 2013, 49: 2451–2453
277 Liu LJ, Zhao CY, Pitts D, Zhao HL, Li Y. CO_2 photoreduction with

H_2O vapor by porous MgO-TiO_2 microspheres: effects of surface MgO dispersion and CO_2 adsorption-desorption dynamics. Catal Sci Technol, 2014, 4: 1539–1546
278 Matějová L, Kočí K, Reli M, *et al.* On sol–gel derived Au-enriched TiO_2 and TiO_2-ZrO_2 photocatalysts and their investigation in photocatalytic reduction of carbon dioxide. Appl Surf Sci, 2013, 285: 688–696
279 Tsuneoka H, Teramura K, Shishido T, Tanaka T. Adsorbed species of CO_2 and H_2 on Ga_2O_3 for the photocatalytic reduction of CO_2. J Phys Chem C, 2010, 114: 8892–8898
280 Teramura K, Iguchi S, Mizuno Y, Shishido T, Tanaka T. Photocatalytic conversion of CO_2 in water over layered double hydroxides. Angew Chem Int Ed, 2012, 51: 8008–8011
281 Morikawa M, Ogura Y, Ahmed N, *et al.* Photocatalytic conversion of carbon dioxide into methanol in reverse fuel cells with tungsten oxide and layered double hydroxide photocatalysts for solar fuel generation. Catal Sci Technol, 2014, 4: 1644–1651
282 Katsumata K, Sakai K, Ikeda K, *et al.* Preparation and photocatalytic reduction of CO_2 on noble metal (Pt, Pd, Au) loaded Zn-Cr layered double hydroxides. Mater Lett, 2013, 107: 138–140
283 Liu L, Zhao C, Li Y. Spontaneous dissociation of CO_2 to CO on defective surface of Cu(I)/TiO_{2-x} NPs at room temperature. J Phys Chem C, 2012, 116: 7904–7912
284 Xie K, Umezawa N, Zhang N, *et al.* Self-doped $SrTiO_{3-\delta}$ photocatalyst with enhanced activity for artificial photosynthesis under visible light. Energy Environ Sci, 2011, 4: 4211–4219
285 Ikeue K, Yamashita H, Anpo M, Takewaki T. Photocatalytic reduction of CO_2 with H_2O on Ti-β zeolite photocatalysts: effect of the hydrophobic and hydrophilic properties. J Phys Chem B, 2001, 105: 8350–8355
286 Ikeue K, Nozaki S, Ogawa M, Anpo M. Photocatalytic reduction of CO_2 with H_2O on Ti-containing porous silica thin film photocatalysts. Catal Lett, 2002, 80: 111–114
287 Niu P, Yang Y, Yu JC, Liu G, Cheng H-M. Switching the selectivity of the photoreduction reaction of carbon dioxide by controlling the band structure of a g-C_3N_4 photocatalyst. Chem Commun, 2014, 50: 10837–10840
288 Lin WY, Frei H. Photochemical CO_2 splitting by metal-to-metal charge-transfer excitation in mesoporous ZrCu(I)-MCM-41 silicate sieve. J Am Chem Soc, 2005, 127: 1610–1611
289 Lin WY, Frei H. Bimetallic redox sites for photochemical CO_2 splitting in mesoporous silicate sieve. CR Chim, 2006, 9: 207–213
290 Hwang J-S, Chang J-S, Park S-E, Ikeue K, Anpo M. Photoreduction of carbondioxide on surface functionalized nanoporous catalysts. Top Catal, 2005, 35: 311–319
291 Li X, Chen X, Li Z. Adsorption equilibrium and desorption activation energy of water vapor on activated carbon modified by an oxidation and reduction treatment. J Chem Eng Data, 2010, 55: 3164–3169
292 Li X, Li H, Huo S, Li Z. Dynamics and isotherms of water vapor sorption on mesoporous silica gels modified by different salts. Kinet Catal, 2010, 51: 754–761
293 Li X, Li Z. Equilibrium and Do–Do model fitting of water adsorption on four commercial activated carbons with different surface chemistry and pore structure. J Chem Eng Data, 2010, 55: 5729–5732
294 Li X, Li W, Zhuang Z, *et al.* Photocatalytic reduction of carbon dioxide to methane over SiO_2-pillared HNb_3O_8. J Phys Chem C, 2012, 116: 16047–16053
295 Yamashita H, Shiga A, Kawasaki S-i, *et al.* Photocatalytic synthesis of CH_4 and CH_3OH from CO_2 and H_2O on highly dispersed active titanium oxide catalysts. Energ Convers Manage, 1995, 36: 617–620
296 Zhang N, Ouyang SX, Li P, *et al.* Ion-exchange synthesis of a micro/mesoporous Zn_2GeO_4 photocatalyst at room temperature for photoreduction of CO_2. Chem Commun, 2011, 47: 2041–2043
297 Yan SC, Ouyang SX, Gao J, *et al.* A room-temperature reactive-template route to mesoporous $ZnGa_2O_4$ with improved photocatalytic activity in reduction of CO_2. Angew Chem Int Ed, 2010, 49: 6400–6404
298 Guo J, Ouyang S, Kako T, Ye J. Mesoporous $In(OH)_3$ for photoreduction of CO_2 into renewable hydrocarbon fuels. Appl Surf Sci, 2013, 280: 418–423
299 Park H-a, Choi JH, Choi KM, Lee DK, Kang JK. Highly porous gallium oxide with a high CO_2 affinity for the photocatalytic conversion of carbon dioxide into methane. J Mater Chem, 2012, 22: 5304–5307
300 Maeda K, Kuriki R, Zhang M, Wang X, Ishitani O. The effect of the pore-wall structure of carbon nitride on photocatalytic CO_2 reduction under visible light. J Mater Chem A, 2014, 2: 15146
301 Lee J, Christopher Orilall M, Warren SC, *et al.* Direct access to thermally stable and highly crystalline mesoporous transition-metal oxides with uniform pores. Nat Mater, 2008, 7: 222–228
302 Sykora M, Kincaid JR. Photochemical energy storage in a spatially organized zeolite-based photoredox system. Nature, 1997, 387: 162–164
303 Anpo M. Photocatalytic reduction of CO_2 with H_2O on highly dispersed Ti-oxide catalysts as a model of artificial photosynthesis. J CO_2 Util, 2013, 1: 8–17
304 Anpo M, Yamashita H, Ikeue K, *et al.* Photocatalytic reduction of CO_2 with H_2O on Ti-MCM-41 and Ti-MCM-48 mesoporous zeolite catalysts. Catal Today, 1998, 44: 327–332
305 Yamashita H, Fujii Y, Ichihashi Y, *et al.* Selective formation of CH_3OH in the photocatalytic reduction of CO_2 with H_2O on titanium oxides highly dispersed within zeolites and mesoporous molecular sieves. Catal Today, 1998, 45: 221–227
306 Ikeue K, Yamashita H, Anpo M. Photocatalytic reduction of CO_2 with H_2O on titanium oxides prepared within the FSM-16 mesoporous zeolite. Chem Lett, 1999, 28: 1135–1136
307 Ikeue K, Mukai H, Yamashita H, *et al.* Characterization and photocatalytic reduction of CO_2 with H_2O on Ti/FSM-16 synthesized by various preparation methods. J Synchrotron Radiat, 2001, 8: 640–642
308 Yang H-C, Lin H-Y, Chien Y-S, Wu J, Wu H-H. Mesoporous TiO_2/SBA-15, and Cu/TiO_2/SBA-15 composite photocatalysts for photoreduction of CO_2 to methanol. Catal Lett, 2009, 131: 381–387
309 Hussain M, Akhter P, Russo N, Saracco G. Novel Ti-KIT-6 material for the photocatalytic reduction of carbon dioxide to methane. Catal Commun, 2013, 36: 58–62
310 Hwang JS, Chang JS, Park SE, Ikeue K, Anpo M. High performance photocatalytic reduction of CO_2 with H_2O by TiSBA-15 mesoporous material. In: Park SE, Chang JS and Lee KW (eds.) Studies in Surface Science and Catalysis. Amsterdam: Elsevier, 2004, 153: 299–302
311 Hamdy MS, Amrollahi R, Sinev I, Mei B, Mul G. Strategies to design efficient silica-supported photocatalysts for reduction of CO_2. J Am Chem Soc, 2014, 136: 594–597
312 Corma A, Fornes V, Pergher SB, Maesen TLM, Buglass JG. Delaminated zeolite precursors as selective acidic catalysts. Nature, 1998, 396: 353–356
313 Varoon K, Zhang X, Elyassi B, *et al.* Dispersible exfoliated zeolite nanosheets and their application as a selective membrane. Science, 2011, 334: 72–75
314 Zhang X, Liu D, Xu D, *et al.* Synthesis of self-pillared zeolite nanosheets by repetitive branching. Science, 2012, 336: 1684–1687
315 Choi M, Na K, Kim J, *et al.* Stable single-unit-cell nanosheets of zeolite MFI as active and long-lived catalysts. Nature, 2009, 461: 246–249
316 Maeda K, Domen K. Photocatalytic water splitting: recent progress and future challenges. J Phys Chem Lett, 2010, 1: 2655–2661
317 Osterloh FE, Parkinson BA. Recent developments in solar water-

splitting photocatalysis. MRS Bull, 2011, 36: 17–22
318 Yang J, Wang D, Han H, Li C. Roles of co-catalysts in photocatalysis and photoelectrocatalysis. Acc Chem Res, 2013, 46: 1900–1909
319 Wang W-N, An W-J, Ramalingam B, *et al.* Size and structure matter: Enhanced CO_2 photoreduction efficiency by size-resolved ultrafine Pt NPs on TiO_2 single crystals. J Am Chem Soc, 2012, 134: 11276–11281
320 Yui T, Kan A, Saitoh C, *et al.* Photochemical reduction of CO_2 using TiO_2: effects of organic adsorbates on TiO_2 and deposition of Pd onto TiO_2. ACS Appl Mater Interfaces, 2011, 3: 2594–2600
321 Zhang XJ, Han F, Shi B, *et al.* Photocatalytic conversion of diluted CO_2 into light hydrocarbons using periodically modulated multiwalled nanotube arrays. Angew Chem Int Ed, 2012, 51: 12732–12735
322 Pathak P, Meziani MJ, Castillo L, Sun YP. Metal-coated nanoscale TiO_2 catalysts for enhanced CO_2 photoreduction. Green Chem, 2005, 7: 667–670
323 Iizuka K, Wato T, Miseki Y, Saito K, Kudo A. Photocatalytic reduction of carbon dioxide over Ag co-catalyst-loaded $ALa_4Ti_4O_{15}$ (A = Ca, Sr, and Ba) using water as a reducing reagent. J Am Chem Soc, 2011, 133: 20863–20868
324 Ran J, Zhang J, Yu J, Jaroniec M, Qiao SZ. Earth-abundant co-catalysts for semiconductor-based photocatalytic water splitting. Chem Soc Rev, 2014, 43: 7787–7812
325 Fukuzumi S, Hong D, Yamada Y. Bioinspired photocatalytic water reduction and oxidation with earth-abundant metal vatalysts. J Phys Chem Lett, 2013, 4: 3458–3467
326 Du P, Eisenberg R. Catalysts made of earth-abundant elements (Co, Ni, Fe) for water splitting: recent progress and future challenges. Energy Environ Sci, 2012, 5: 6012–6021
327 Yamashita H, Nishiguchi H, Kamada N, *et al.* Photocatalytic reduction of CO_2 with H_2O on TiO_2 and Cu/TiO_2 catalysts. Res Chem Intermediat, 1994, 20: 815–823
328 Liu D, Fernández Y, Ola O, *et al.* On the impact of Cu dispersion on CO_2 photoreduction over Cu/TiO_2. Catal Commun, 2012, 25: 78–82
329 Lee DS, Chen HJ, Chen YW. Photocatalytic reduction of carbon dioxide with water using $InNbO_4$ catalyst with NiO and Co_3O_4 co-catalysts. J Phys Chem Solids, 2012, 73: 661–669
330 Li R, Zhang F, Wang D, *et al.* Spatial separation of photogenerated electrons and holes among {010} and {110} crystal facets of $BiVO_4$. Nat Commun, 2013, 4: 1432
331 Barber J. Photosynthetic energy conversion: natural and artificial. Chem Soc Rev, 2009, 38: 185–196
332 Fillol JL, Codolà Z, Garcia-Bosch I, *et al.* Efficient water oxidation catalysts based on readily available iron coordination complexes. Nat Chem, 2011, 3: 807–813
333 Toma FM, Sartorel A, Iurlo M, *et al.* Efficient water oxidation at carbon nanotube–polyoxometalate electrocatalytic interfaces. Nat Chem, 2010, 2: 826–831
334 Yin Q, Tan JM, Besson C, *et al.* A Fast soluble carbon-free molecular water oxidation catalyst based on abundant metals. Science, 2010, 328: 342–345
335 Liang Y, Li Y, Wang H, Dai H. Strongly coupled inorganic/nanocarbon hybrid materials for advanced electrocatalysis. J Am Chem Soc, 2013, 135: 2013–2036
336 Kanan MW, Nocera DG. *In situ* formation of an oxygen-evolving catalyst in neutral water containing phosphate and Co^{2+}. Science, 2008, 321: 1072–1075
337 Hurst JK. In pursuit of water oxidation catalysts for solar fuel production. Science, 2010, 328: 315–316
338 Rajalakshmi K, Jeyalakshmi V, Krishnamurthy K, Viswanathan B. Photocatalytic reduction of carbon dioxide by water on titania: role of photophysical and structural properties. Indian J Chem A, 2012, 51: 411
339 Pan J, Wu X, Wang LZ, *et al.* Synthesis of anatase TiO_2 rods with dominant reactive {010} facets for the photoreduction of CO_2 to CH_4 and use in dye-sensitized solar cells. Chem Commun, 2011, 47: 8361–8363
340 Ogura K, Kawano M, Yano J, Sakata Y. Visible-light-assisted decomposition of H_2O and photomethanation of CO_2 over CeO_2-TiO_2 catalyst. J Photoch Photobio A, 1992, 66: 91–97
341 Sayama K, Arakawa H. Photocatalytic decomposition of water and photocatalytic reduction of carbon dioxide over zirconia catalyst. J Phys Chem, 1993, 97: 531–533
342 Takayama T, Tanabe K, Saito K, Iwase A, Kudo A. The $KCaSrTa_5O_{15}$ photocatalyst with tungsten bronze structure for water splitting and CO_2 reduction. Phys Chem Chem Phys, 2014, 16: 24417–24422
343 Li K, Handoko AD, Khraisheh M, Tang J. Photocatalytic reduction of CO_2 and protons using water as an electron donor over potassium tantalate nanoflakes. Nanoscale, 2014, 6: 9767–9773
344 Zhai Q, Xie S, Fan W, *et al.* Photocatalytic conversion of carbon dioxide with water to methane: platinum and copper(I) oxide co-catalysts with a core–shell structure. Angew Chem Int Ed, 2013, 52: 5776–5779
345 Reece SY, Hamel JA, Sung K, *et al.* Wireless solar water splitting using silicon-based semiconductors and earth-abundant catalysts. Science, 2011, 334: 645–648
346 Smith RDL, Prévot MS, Fagan RD, *et al.* Photochemical route for accessing amorphous metal oxide materials for water oxidation catalysis. Science, 2013, 340: 60–63
347 Rosen J, Hutchings GS, Jiao F. Ordered mesoporous cobalt oxide as highly efficient oxygen evolution catalyst. J Am Chem Soc, 2013, 135: 4516–4521
348 Cobo S, Heidkamp J, Jacques P-A, *et al.* A Janus cobalt-based catalytic material for electro-splitting of water. Nat Mater, 2012, 11: 802–807
349 Liang Y, Li Y, Wang H, *et al.* Co_3O_4 nanocrystals on graphene as a synergistic catalyst for oxygen reduction reaction. Nat Mater, 2011, 10: 780–786
350 Dimitrijevic NM, Shkrob IA, Gosztola DJ, Rajh T. Dynamics of interfacial charge transfer to formic acid, formaldehyde, and methanol on the surface of TiO_2 NPs and its role in methane production. J Phys Chem C, 2011, 116: 878–885
351 Yang XY, Xiao TC, Edwards PP. The use of products from CO_2 photoreduction for improvement of hydrogen evolution in water splitting. Int J Hydrogen Energ, 2011, 36: 6546–6552
352 Kim W, Seok T, Choi W. Nafion layer-enhanced photosynthetic conversion of CO_2 into hydrocarbons on TiO_2 NPs. Energy Environ Sci, 2012, 5: 6066–6070
353 Pathak P, Meziani MJ, Li Y, Cureton LT, Sun YP. Improving photoreduction of CO_2 with homogeneously dispersed nanoscale TiO_2 catalysts. Chem Commun, 2004, 1234–1235
354 Premkumar J, Ramaraj R. Photocatalytic reduction of carbon dioxide to formic acid at porphyrin and phthalocyanine adsorbed Nafion membranes. J Photoch Photobio A, 1997, 110: 53–58
355 Premkumar JR, Ramaraj R. Photoreduction of carbon dioxide by metal phthalocyanine adsorbed Nafion membrane. Chem Commun, 1997, 343–344
356 Ampelli C, Centi G, Passalacqua R, Perathoner S. Synthesis of solar fuels by a novel photoelectrocatalytic approach. Energy Environ Sci, 2010, 3: 292–301
357 Cheng J, Zhang M, Wu G, *et al.* Photoelectrocatalytic reduction of CO_2 into chemicals using Pt-modified reduced graphene oxide combined with Pt-modified TiO_2 nanotubes. Environ Sci Technol, 2014, 48: 7076–7084
358 Qin GH, Zhang Y, Ke XB, *et al.* Photocatalytic reduction of carbon dioxide to formic acid, formaldehyde, and methanol using dye-sensitized TiO_2 film. Appl Catal B-Environ, 2013, 129: 599–605
359 Morikawa M, Ahmed N, Ogura Y, Izumi Y. Polymer electrolyte fuel

cell supplied with carbon dioxide. Can be the reductant water instead of hydrogen? Appl Catal B-Environ, 2012, 117-118: 317–320
360 Yang CC, Yu YH, van der Linden B, Wu JCS, Mul G. Artificial photosynthesis over crystalline TiO_2-based catalysts: fact or fiction? J Am Chem Soc, 2010, 132: 8398–8406

Acknowledgment Li X would like to thank the National Natural Science Foundation of China (NSFC) (20906034), the project (2015-KF-7) supported by State Key Laboratory of Advanced Technology for Material Synthesis and Processing (Wuhan University of Technology) and the Key Academic Program of the 3rd phase "211 Project" of South China Agricultural University (2009B010100001) for their support. Yu J would like to thank the State Key Project of Fundamental Research for Nanoscience and Nanotechnology (2013CB632402), and NSFC (51272199, 51320105001 and 21433007) and Deanship Of Scientific Research (DSR) of King Abdulaziz University (90-130-35-HiCi). Fang Y. would like to thank NSFC (20963002 and 21173088) for their support.

Author contributions Li X wrote the paper; Low J prepared the figures; Yu J provided the overall concept and revised manuscript; Wen J and Fang Y classified and analyzed the reference papers. All authors participated in the discussion.

Conflict of interest The authors declare that they have no conflict of interest.

Xin Li received his BSc and PhD degrees in chemical engineering from Zhengzhou University in 2002 and South China University of Technology in 2007, respectively. Then, he joined South China Agricultural University as a faculty staff member, and became an associate professor of applied chemistry in 2011. During 2012–2013, he worked as a visiting scholar at the Electrochemistry Center, the University of Texas at Austin, USA. His research interests include photocatalysis, photoelectrochemistry, adsorption and the related materials and devices development.

Jiaguo Yu received his BSc and MSc in chemistry from Huazhong Normal University and Xi'an Jiaotong University, respectively, and his PhD in materials science in 2000 from Wuhan University of Technology (WUT). In 2000, he became a professor of WUT. He was a post-doctor of the Chinese University of Hong Kong from 2001 to 2004, visiting scientist from 2005 to 2006 at the University of Bristol, and visiting scholar from 2007 to 2008 at the University of Texas at Austin, USA. His research interests include semiconductor photocatalysis, dye-sensitized solar cells and so on.

中文摘要 近年来, 严重的化石燃料短缺以及环境污染问题使得人工光合作用引起了科研工作者的广泛关注, 光催化转换CO_2成为有价值的太阳能燃料被认为是解决能源危机以及环境问题的最好的方法之一. 有效地控制半导体表面的催化反应以及光生载流子是制备高活性以及高选择性半导体CO_2还原光催化剂的关键因素, 至今, 研究人员已经提出了许多策略来增强光催化转换CO_2的活性以及选择性. 本文在分析提高光催化效率和选择性限制因素的基础上, 尝试从几个不同方面总结了近些年来提高光催化CO_2还原效率的方法以及它们的设计原理, 包括增强半导体可见光响应、促进光生电子空穴分离、提高CO_2的吸附和活化、加速CO_2还原的动力学以及抑制不良反应等方面. 因此, 本文不仅系统地总结了近年来高活性高选择性光催化CO_2还原光催化剂的设计进展, 而且为高效光解水产氢和污染物降解光催化剂的设计提供了重要参考.